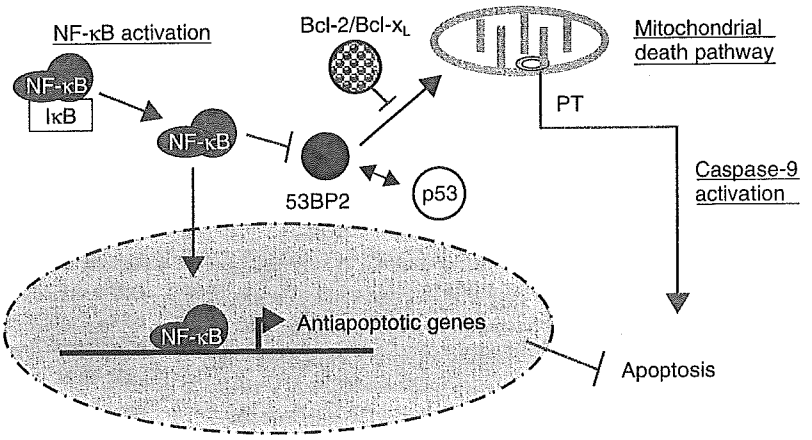

Figure 6 Regulation of the 53BP2S-mediated apoptosis by NF-κB and Bcl-2/Bcl-X_L. Previous findings indicate that p53 interacts with 53BP2 proteins to activate the proapoptotic action. Our findings indicate that NF-κB and Bcl-2/Bcl-X_L appear to block this action of 53BP2S/Bbp. The selective action of 53BP2S/Bbp with these proteins may determine the threshold of the cellular susceptibility to the intrinsic death pathway. See Discussion for the details.

San Diego, CA, USA), and rabbit polyclonal antibody to human p65 (Santa Cruz Biotech, Santa Cruz, CA, USA), goat polyclonal antibody to human p50 (Santa Cruz Biotech) were purchased from individual suppliers. The rabbit polyclonal antibody to human 53BP2 was a generous gift from L. Naumovski (Stanford University, CA, USA). Mouse monoclonal antibodies to caspase-8 (cleaved form) and caspase-9 (cleaved form) and rabbit polyclonal antibody to PARP were purchased from Cell Signaling Technology (Beverly, MA, USA).

Plasmids

Construction of the 53BP2S/Bbp expression plasmids, pcDNA3.1–53BP2 and pEGFP-53BP2, expressing 53BP2S/Bbp protein (1005 amino acids) either alone or in fusion with green fluorescence protein (GFP), was reported previously (Yang *et al.* 1999). Human bcl-2, bcl-x_L, and bclx_L mutant (ΔBH4) cDNAs were subcloned into the pUC-CAGGS expression vector as previously described (Shimizu *et al.* 1996, 2000).

Cell lines and cultures

The 53BP2S/Bbp inducible cell line 293/53BP2 and its control cell line 293/LZ were kindly provided by Charles D. Lopez, Stanford University, CA, USA and previously described (Lopez *et al.* 2000). These cells were grown at 37 °C in 5% CO_2 in Dulbecco's modified Eagle medium (DMEM) with 10% (v/v) heat-inactivated fetal calf serum, 290 μg/mL of L-glutamine, 100 U/mL penicillin, 100 μg/mL streptomycin, 600 μg/mL G418 and 500 μg/mL Zeocin. A human pancreatic cancer cell line MIA PaCa-2 was grown in Eagle minimal essential medium supplemented with nonessential amino acids, 10% (v/v) heat-inactivated fetal calf serum, 100 U/mL penicillin, and 100 μg/mL streptomycin.

Microscopic examination

In order to examine the apoptotic cell morphology, 293/53BP2 cells were cultured on 2-well Laboratory-Tek tissue culture chamber slides (Nunc, Inc., Naperville, IL, USA) and stimulated by pon A. The cells were fixed with 4.0% paraformaldehyde in PBS for 15 min at room temperature, rinsed twice in PBS and stained with Hoechst-33258. The apoptotic cells were identified by their shrunken morphology and the condensed and fragmented nuclear morphology.

Evaluation of apoptosis by Western blotting

Apoptosis was also assessed by the cleavage of PARP, and caspases-8 and -9 by Western blotting using relevant antibodies described above. Briefly, whole cell extracts were lyzed in 200 μL of ice-cold lysis buffer (50 mM Tris-HCl (pH 8.0), 100 mM NaCl, 5 mM EDTA, 50 mM sodium fluoride, 2 mM dithiothreitol, 0.25% Nonidet P-40, 1 mM phenylmethyl-sulfonyl fluoride, 10 μg/mL aprotinin, 10 μg/mL leupeptin and 1 μg/mL pepstatin A). The lysate was cleared by centrifugation and the protein concentration of the whole cell extract was measured using Bio-Rad DC protein assay kit (Bio-Rad). Equal amounts of cell lysates (10 μg protein) were resolved by 10% SDS-PAGE and transferred on nitrocellulose membrane followed by incubating with individual antibodies. The immumoreactive proteins were visualized by ECL (Asamitsu *et al.* 2003).

Determination of mitochondrial ΔΨm in cultured cells

To visualize the cells with depressed ΔΨm, cells growing on Laboratory-TekII chambered cover glass were stained with 40 nM CMX-Ros in PBS for 15 min, washed with PBS three times and observed under the confocal microscope (Bio-Rad MRC600UVF). The acquisitions of the mitochondrial images were provided by 585LP emission filter with same setting (Iris: 2.0, Gain: 1.4).

Cell survival assay

To quantitatively measure the cell survival, cell cultures were stained with trypan blue and counted under microscopy in triplicates. To

determine the anti-apoptotic effect of NF-κB, 293/53BP2 cells were cultured without pon A to 50% confluence, stimulated with pon A (5 μM), and after 24 h in culture they were treated with IL-1β (20 ng/mL). The cell survival was assessed every 24 h for an additional 4 days after the stimulation with IL-1β.

Electrophoretic mobility shift assay (EMSA)

293/53BP2 cells were pretreated with or without IL-1β (20 ng/mL) and nuclear extracts were prepared as previously described (Takada *et al.* 2002). The double-stranded oligonucleotide probe for NF-κB was synthesized and end-labeled by γ-[^{32}P]-dATP. The κB sequence was taken from the human immunodeficiency virus long-terminal repeat (HIV-LTR). The κB sequence used was forward (5′-TTT CTA GGG ACT TTC CGC CTG GGG ACT TTC CAG-3′) and complement (5′-TTT CTG GAA AGT CCC CAG GCG GAA AGT CCC TAG-3′). Nuclear extracts were incubated in 10 μL EMSA buffer containing the radiolabelled κB oligonucleotide probe. The samples were analyzed by 6% non-denaturing PAGE. For NF-κB supershift assay, antibodies to NF-κB p65 and/or p50 subunits were added (30 min, 4 °C).

Acknowledgements

We thank Dr. Louie Naumovski (Stanford University) for the generous gifts of 293/53BP2 cells and polyclonal antibody to 53BP2S/Bbp. This work was supported in part by Grants-in-Aid from the Ministry of Health, Labor and Welfare, and the Ministry of Education, Culture, Sports, Science and Technology of Japan, and Japanese Human Sciences Foundation.

References

Ao, Y., Rohde, L.H. & Naumovski, L. (2001) p53-interacting protein 53BP2 inhibitsclonogenic survival and sensitizes cells to doxorubicin but not paclitaxel-induced apoptosis. *Oncogene* **20**, 2720–2725.

Arlt, A., Vorndamm, J., Müerköster, S., *et al.* (2002) Autocrine production of interleukin 1beta confers constitutive nuclear factor κB activity and chemoresistance in pancreatic carcinoma cell lines. *Cancer Res.* **62**, 910–916.

Asamitsu, K., Kanazawa, S., Tetsuka, T. & Okamoto, T. (2003) RING finger protein AO7 supports NF-kappaB-mediated transcription by interacting with the transactivation domain of the p65 subunit. *J. Biol. Chem.* **278**, 26879–26887.

Bergamaschi, D., Samuels, Y., Jin, B., Duraisingham, S., Crook, T. & Lu, X. (2004) ASPP1 and ASPP2: common activators of p53 family members. *Mol. Cell. Biol.* **24**, 1341–1350.

Bottero, V., Rossi, F., Samson, M., Mari, M., Hofman, P. & Peyron, J.F. (2001) IκBα, the NF-κB inhibitory subunit, interacts with ANT, the mitochondrial ATP/ADP translocator. *J. Biol. Chem.* **276**, 21317–21324.

Chen, C., Edelstein, L.C. & Gelinas, C. (2000) The Rel/NF-κB family directly activates expression of the apoptosis inhibitor Bcl-X_L. *Mol. Cell. Biol.* **20**, 2687–2695.

Chen, F., Castranova, V. & Shi, X. (2001) New insights into the role of nuclear factor-κB in cell growth regulation. *Am. J. Pathol.* **159**, 387–397.

Chu, Z.L., McKinsey, T.A., Liu, L., Gentry, J.J., Malim, M.H. & Ballard, D.W. (1997) Suppression of tumor necrosis factor-induced cell death by inhibitor of apoptosis c-IAP2 is under NF-κB control. *Proc. Natl. Acad. Sci. USA* **94**, 10057–10062.

Cogswell, P.C., Kashatus, D.F., Keifer, J.A., *et al.* (2003) NF-κB and IκBα are found in the mitochondria. Evidence for regulation of mitochondrial gene expression by NF-κB. *J. Biol. Chem.* **278**, 2963–2968.

Daniel, N.N. & Korsmeyer, S.J. (2004) Cell death: critical control points. *Cell* **116**, 205–219.

DeLuca, C., Kwon, H., Pelletier, N., Wainberg, M.A. & Hiscott, J. (1998) NF-κB protects HIV-1-infected Myeloid cells from apoptosis. *Virology* **244**, 27–38.

Gorina, S. & Pavletich, N.P. (1996) Structure of the p53 tumor suppressor bound to the ankyrin and SH3 domains of 53BP2. *Science* **274**, 1001–1005.

Haddad, J.J. (2004) On the antioxidation mechanisms of Bcl-2: a retrospective of NF-κB signaling and oxidative stress. *Biochem. Biophys. Res. Commun.* **322**, 355–363.

Iwabuchi, K., Bartel, P.L., Li, B., Marraccino, R. & Fields, S. (1994) Two cellular proteins that bind to wild-type but not mutant p53. *Proc. Natl. Acad. Sci. USA* **91**, 6098–6102.

Iwabuchi, K., Li, B., Massa, H.F., Trask, B.J., Date, T. & Fields, S. (1998) Stimulation of p53-meditated transcriptional activation by the p53-binding proteins, 53BP1 and 53BP2. *J. Biol. Chem.* **273**, 26061–26068.

Kajino, S., Suganuma, M., Teranishi, F., *et al.* (2000) Evidence that de novo protein synthesis is dispensable for anti-apoptotic effects of NF-κB. *Oncogene* **19**, 2233–2239.

Karin, M. & Lin, A. (2002) NF-κB at the crossroads of like and death. *Nature Immunol.* **3**, 221–227.

Kobayashi, S., Kajino, S., Takahashi, N., *et al.* (2005) 53BP2 induces apoptosis through the mitochondrial death pathway. *Genes Cells* **3**, 253–260.

Lopez, C.D., Ao, Y., Rohde, L.H., *et al.* (2000) Proapoptotic p53-interacting protein 53BP2 is induced by UV irradiation but suppressed by p53. *Mol. Cell. Biol.* **20**, 8018–8025.

Mori, T., Okamoto, H., Takahashi, N., Ueda, R. & Okamoto, T. (2000) Aberrant overexpression of 53BP2 mRNA in lung cancer cell lines. *FEBS Lett.* **465**, 124–128.

Naumovski, L. & Cleary, M.L. (1996) The p53-binding protein 53BP2 also interacts with Bc12 and impedes cell cycle progression at G2/M. *Mol. Cell. Biol.* **16**, 3884–3892.

Samuels-Lev, Y., O'Connor, D.J., Bergamaschi, D., *et al.* (2001) ASPP proteins specifically stimulate the apoptotic function of p53. *Mol. Cell* **8**, 781–794.

Shimizu, S., Eguchi, Y., Kamiike, W., *et al.* (1996) Bcl-2 blocks loss of mitochondrial membrane potential while ICE inhibitors act at a different step during inhibition of death induced by respiratory chain inhibitors. *Oncogene* **13**, 21–29.

Shimizu, S., Konishi, A., Kodama, T. & Tsujimoto, Y. (2000) BH4 domain of antiapoptotic Bcl-2 family members closes voltage-dependent anion channel and inhibits apoptotic

mitochondrial changes and cell death. *Proc. Natl. Acad. Sci. USA* **97**, 3100–3105.

Takada, N., Sanda, T., Okamoto, H., *et al.* (2002) RelA-associated inhibitor blocks transcription of human immunodeficiency virus type1 by inhibiting NF-κB and Sp1 actions. *J. Virol.* **76**, 8019–8030.

Takahashi, N., Kobayashi, S., Jiang, X., *et al.* (2004) Expression of 53BP2 and ASPP2 proteins from TP53BP2 gene by alternative splicing. *Biochem. Biophys. Res. Commun.* **315**, 434–438.

Wu, M.X., Ao, Z., Prasad, K.V., Wu, R. & Schlossman, S.F. (1998) IEX-1L, an apoptosis inhibitor involved in NF-κB-mediated cell survival. *Science* **281**, 998–1001.

Yang, J.P., Ono, T., Sonta, S., Kawabe, T. & Okamoto, T. (1997) Assignment of p53 binding protein (TP53BP2) to human chromosome band 1q42.1 by in situ hybridization. *Cytogenet. Cell Genet.* **78**, 61–62.

Yang, J.P., Hori, M., Takahashi, N., Kawabe, T., Kato, H. & Okamoto, T. (1999) NF-κB subunit p65 binds to 53BP2 and inhibits cell death induced by 53BP2. *Oncogene* **18**, 5177–5186.

Yoshikawa, H., Nagashima, M., Khan, M.A., McMenamin, M.G., Hagiwara, K. & Harris, C.C. (1999) Mutational analysis of p73 and p53 in human cancer cell lines. *Oncogene* **18**, 3415–3421.

Received: 27 January 2005
Accepted: 05 May 2005

THE JOURNAL OF BIOLOGICAL CHEMISTRY
© 2005 by The American Society for Biochemistry and Molecular Biology, Inc.

Vol. 280, No. 29, Issue of July 22, pp. 26701–26713, 2005
Printed in U.S.A.

Induction of *OGG1* Gene Expression by HIV-1 Tat*

Received for publication, March 25, 2005, and in revised form, June 1, 2005
Published, JBC Papers in Press, June 1, 2005, DOI 10.1074/jbc.M503313200

Kenichi Imai‡, Kenji Nakata‡, Kazuaki Kawai§, Takaichi Hamano¶, Nan Mei§, Hiroshi Kasai§, and Takashi Okamoto‡‖

From the ‡Department of Molecular and Cellular Biology, Nagoya City University Graduate School of Medical Sciences, 1 Kawasumi, Mizuho-cho, Mizuho-ku, Nagoya, Aichi 467-8601, the §Department of Environmental Oncology, Institute of Industrial Ecological Sciences, University of Occupational and Environmental Health, Kitakyushu, Fukuoka 807-8555, and the ¶AIDS Research Center, National Institute of Infectious Diseases, 1-23-1 Toyama, Shinjuku-ku, Tokyo 162-8640, Japan

To identify the cellular gene target for Tat, we performed gene expression profile analysis and found that Tat up-regulates the expression of the *OGG1* (8-oxoguanine-DNA glycosylase-1) gene, which encodes an enzyme responsible for repairing the oxidatively damaged guanosine, 8-oxo-7,8-dihydro-2′-deoxyguanosine (8-oxo-dG). We observed that Tat induced *OGG1* gene expression by enhancing its promoter activity without changing its mRNA stability. We found that the upstream AP-4 site within the *OGG1* promoter is responsible and that Tat interacted with AP-4 and removed AP-4 from the *OGG1* promoter by *in vivo* chromatin immunoprecipitation assay. Thus, Tat appears to activate *OGG1* expression by sequestrating AP-4. Interestingly, although Tat induces oxidative stress known to generate 8-oxo-dG, which causes the G:C to T:A transversion, we observed that the amount of 8-oxo-dG was reduced by Tat. When *OGG1* was knocked down by small interfering RNA, Tat increased the amount of 8-oxo-dG, thus confirming the role of OGG1 in preventing the formation of 8-oxo-dG. These findings collectively indicate the possibility that Tat may play a role in maintenance of the genetic integrity of the proviral and host cellular genomes by up-regulating OGG1 as a feed-forward mechanism.

Tat is an essential transactivator of human immunodeficiency virus (HIV)[1] gene expression and viral replication (1). Tat stimulates viral gene expression by directly binding to the characteristic RNA stem-loop-bulge structure called the transactivation response region located within the long terminal repeat (2, 3) and enhancing the processivity of RNA polymerase II (4, 5). The transcriptional activity of Tat is supported by interaction with cellular factors such as positive transcription elongation factor-b (6–8) and histone acetyltransferase (9). Cyclin T1, a regulatory subunit of the positive transcription elongation factor-b complex, binds to the activation domain of Tat and facilitates the hyperphosphorylation of the C-terminal domain of RNA polymerase II at the vicinity of HIV genes. Thus, Tat makes RNA polymerase II highly competent for the transcription elongation and productive expression of HIV genes (10).

Although much of the efforts in Tat studies have focused on its transcriptional activation from the HIV provirus, the actions of Tat on cellular genes have also been revealed. For example, Tat is known to promote cellular transformation (11), to induce oxidative stress (12, 13), and to elicit inflammatory reactions (14, 15). Choi *et al.* (16) observed that Tat transgenic mice exhibit decreased gene expression of the γ-glutamylcysteine synthetase regulatory subunit and decreased GSH content in tissues. These biological actions of Tat are considered to cause activation of nuclear factor-κB, AP-1 (activating protein-1), and mitogen-activated protein kinase (13, 17). These findings prompted us to search for cellular target genes of Tat, either up-regulated or down-regulated, using a gene expression profile analysis.

In addition to the very high efficiency of the viral replication rate that is mainly ascribable to Tat action, HIV owes its morbidity to its high mutation rate, leading to the emergence of drug resistance and escape from the host immune response. In fact, the high frequency of G:C to A:T and G:C to T:A mutations was previously observed in HIV-1 and other lentiviruses (18–21). Recent studies (22–25) have deciphered one such mechanism that involves the HIV-encoded virion infectivity factor blocking the enzymatic activity of cytidine deaminase CEM15 (also known as APOBEC3G for apolipoprotein B mRNA-editing enzyme, catalytic polypeptide-like 3G), which induces G:C to A:T hypermutation in newly synthesized DNA. Another type of mutation, G:C to T:A transversion, is mediated by the generation of 8-oxo-7,8-dihydro-2′-deoxyguanosine (8-oxo-dG) by radical oxygen species (ROS) and occurs at the DNA level (26, 27). The oxidatively damaged guanosine, 8-oxo-dG, is widely accepted as a pre-mutagenic lesion because of its potential to mispair with adenine, thus generating the G:C to T:A transversion. This type of mutation is often found in tumor suppressor genes and oncogenes, such as p53 and K-*ras*, in mammalian cells (28, 29). The OGG1 (8-oxoguanine-DNA glycosylase-1) enzyme is responsible for the excision/repair of this oxidatively damaged DNA by excising 8-oxo-dG (30–32). In fact, *OGG1* gene knockout actually shows accumulation of such a mutation (33, 34).

In this study, we demonstrate the up-regulation of OGG1 by Tat and provide evidence that this effect of Tat is through the sequestration of the negative transcription factor AP-4 for the expression of *OGG1*. We examine the effect of Tat on the actual

* This work was supported in part by grants-in-aid from the Ministry of Health, Labor, and Welfare of Japan, the Ministry of Education, Culture, Sports, Science, and Technology of Japan, and the Japanese Health Sciences Foundation. The costs of publication of this article were defrayed in part by the payment of page charges. This article must therefore be hereby marked "*advertisement*" in accordance with 18 U.S.C. Section 1734 solely to indicate this fact.

‖ To whom correspondence should be addressed. Tel.: 81-52-853-8204; Fax: 81-52-859-1235; E-mail: tokamoto@med.nagoya-cu.ac.jp.

[1] The abbreviations used are: HIV, human immunodeficiency virus; 8-oxo-dG, 8-oxo-7,8-dihydro-2′-deoxyguanosine; ROS, radical oxygen species; siRNA, small interfering RNA; mTat, mutant Tat; PonA, ponasterone A; PBMCs, peripheral blood mononuclear cells; RT, reverse transcription; PBS, phosphate-buffered saline; ChIP, chromatin immunoprecipitation; HPLC, high performance liquid chromatography; ECD, electrochemical detector.

levels of 8-oxo-dG in the presence and absence of small interfering RNA (siRNA) against *OGG1* mRNA.

EXPERIMENTAL PROCEDURES

Plasmids—The cDNA of wild-type Tat (101 amino acids) originating from HIV-1 was amplified by PCR with the oligonucleotide primer pair 5′-CGC GGA TCC GCG CCA CCA TGG ATT ACA AGG ATG ACG ACG ATA AGA TGG AGC CAG TAG ATC CTA GAC TAG AGC CCT GG-3′ (forward; containing an EcoRI site and a FLAG epitope) and 5′-CCG GAA TTC CGG CTG ATG GAC CGG ATC TGT CTC-3′ (reverse; containing a BamHI site). The amplified DNA fragment was digested with EcoRI and BamHI and ligated in-frame into the pIND-V5 expression vector (Invitrogen), thus generating pIND-Tat. As a control, we employed mutant Tat (mTat) lacking transcriptional activity because of the absence of binding activity with cyclin T1 or the transactivation response region (6–8). The plasmid expressing mutant Tat (pIND-mTat) in which Cys^{30} and Lys^{41} were substituted with Ala was generated using a QuikChange site-directed mutagenesis kit (Stratagene) with the following mutagenic oligonucleotide primer pairs: 5′-CTA TTG TAA AAA GGC CTG CTT TCA TTG CC-3′ (forward) and 5′-GGC AAT GAA AGC AGG CCT TTT TAC AAT AG-3′ (reverse) or 5′-GTT TCA CAA CAG CCG CCT TAG GCA TC-3′ (forward) and 5′-GAT GCC TAA GGC GGC TGT TGT GAA AC-3′ (reverse). To generate the mammalian expression plasmid for AP-4, AP-4 gene was amplified by PCR with the oligonucleotide primer pair 5′-CGC GGA TCC GCG CCA CCA TGG ATT ACA AGG ATG ACG ACG ATA AGA TGG AGC CAG TAG ATC CTA GAC TAG AGC CCT GG-3′ (forward; containing an EcoRI site) and 5′-CCG GAA TTC CGG CTG ATG GAC CGG ATC TGT CTC-3′ (reverse; containing a BamHI site). The amplified DNA fragment was digested with EcoRI and BamHI and ligated in-frame into the pcDNA-Myc expression vector (Invitrogen). The construction of pCD12-luc, containing the HIV-1 long terminal repeats V3 and R linked to the luciferase gene, and pcDNA-Tat was described previously (35, 36). Human *OGG1* promoter-luciferase fusion constructs, including pPR116, pPR128, pPR130, and pPR143, were kindly provided by Dr. J. P. Radicella (Radiobiologie Moleculaire et Cellulaire, CNRS-CEA, Fontenay aux Roses, France) (37). The mutant pPR128-luc reporter constructs were generated using a QuikChange site-directed mutagenesis kit. The mutant sequences (sense strand) utilized were as follows: 5′-AP-4 site mutant (m5′AP-4), GAC GGC AGG CAG tcg cga TGG CGG CCG GCG; 3′-AP-4 site mutant (m3′AP-4), GGG AAA GGC GAG tcg cga GCA GAG AGC CCA G; GA TA site mutant (mGATA), CTT GCA GCC Tct TAG TTA AGA TAC AGC; and AP-2 site mutant (mAP-2), CAG CTG TGG CGG CCa ttC GGG ACG ACA ATC (with consensus binding sites underlined and mutated sequences in lowercase letters). The construct containing mutations in both the 5′- and 3′-AP-4 sites (mwAP-4) was generated by two successive PCRs using the m5′AP-4 and m3′AP-4 mutant sequences. The control luciferase reporter plasmid pGL3-Basic vector was purchased from Promega. All constructs were confirmed by dideoxynucleotide sequencing using an ABI PRISM™ dye terminator cycle sequencing ready kit (PerkinElmer Life Sciences) on an Applied Biosystems 313 Automated DNA Sequencer.

Cell Lines That Inducibly Express Tat, mTat, and LacZ—HEK293-EcR cells, stably transfected with pVgRXR expressing the ecdysone receptor, were purchased from Invitrogen and transfected with pIND-Tat and pIND-mTat to establish Tat/293 and mTat/293 cells, respectively. The control cell line (LacZ/293) was a gift from Dr. L. Naumovski (Stanford University, Stanford, CA) (38). Expression of these genes is under the stringent control of a homolog of the insect hormone 20-OH-ecdysone, ponasterone A (PonA; Invitrogen). Cells containing these plasmids were selected by 500 μg/ml G418 and 450 μg/ml Zeocin. Cell clones were singly isolated by two successive rounds of limiting dilution of cells and were screened for the expression and transcriptional activity of Tat proteins.

Cell Culture—Tat/293, mTat/293, and LacZ/293 cells were grown at 37 °C in Dulbecco's modified Eagle's medium (Sigma) with 10% heat-inactivated fetal bovine serum (Immuno-Biological Laboratories, Maebashi, Japan), 100 units/ml penicillin, and 100 μg/ml streptomycin. The Jurkat T cell line was maintained in RPMI 1640 medium (Sigma) with 10% fetal bovine serum, penicillin, and streptomycin. Peripheral blood mononuclear cells (PBMCs) were isolated from healthy donors, stimulated with phytohemagglutinin for 48 h, and further cultured in RPMI 1640 medium supplemented with 10% heat-inactivated fetal bovine serum and 20 units/ml interleukin-2.

Preparation of mRNA—Total cellular RNA was prepared from each cell clone using RNeasy (Qiagen Inc.). Purification of polyadenylated mRNA was carried out using an Oligotex-dT30 super RNA purification kit (Takara, Ohtsu, Japan) as described previously (39, 40). The mRNA samples were digested with RNase-free DNase, ethanol-precipitated, and further purified through Microcon YM-100 columns (Amicon Inc.). The quantity and quality of mRNA were assessed by capillary electrophoresis using an Agilent 2100 bioanalyzer.

Generation of Fluorescently Tagged cDNA and Gene Expression Profile Analysis—Gene expression profiles were examined as described (39, 40) using the human 3K DNA CHIP™ (Takara) containing 2600 human genes of known functions. Briefly, fluorescently labeled cDNA was synthesized from 1-μg aliquots of purified mRNA by oligo(dT)-primed polymerization using SuperScript II reverse transcriptase (Invitrogen). The pool of nucleotides in the labeling reaction contained 0.5 mM each dGTP, dATP, and dTTP; 0.3 mM dCTP; and 0.1 mM fluorescent nucleotide (Cy3- or Cy5-labeled dCTP, Amersham Biosciences). Fluorescently labeled cDNA was purified by chromatography through Microcon YM-20 columns (Amicon Inc.). The microarray slide was hybridized to combined Cy5-dCTP- and Cy3-dCTP-labeled cDNA probes for 14 h in hybridization solution (6× SSC and 0.2% SDS with 5× Denhardt's solution and carrier DNA) at 65 °C under coverslips. After hybridization, the microarray slide was washed twice with 1.2× SSC and 0.2% SDS at 55 °C for 5 min, with 1.2× SSC and 0.2% SDS at 65 °C for 5 min, and with 0.05× SSC at room temperature as a final wash. The hybridized array was scanned at 10-μm resolution on an Affymetrix 428 array scanner. Analysis of differential expression of each gene was performed using ImaGene Version 4.2 computer software (Bio-Discovery Ltd.). Normalization of hybridized signals was performed by global scaling. These experiments were repeatedly performed; we performed comparative microarray analyses three times (24 h after PonA stimulation in 293/Tat and 293/LacZ cells) and two times (12 h after PonA stimulation in 293/Tat and 293/LacZ cells).

Co-immunoprecipitation and Immunoblot Assay—The experimental procedures have been described previously (41). Briefly, cells were harvested with lysis buffer (25 mM HEPES-NaOH (pH 7.9), 150 mM NaCl, 1.5 mM $MgCl_2$, 0.2 mM EDTA, 0.3% Nonidet P-40, 1 mM dithiothreitol, and 0.5 mM phenylmethylsulfonyl fluoride). The lysates were cleared by centrifugation, and the supernatants were incubated overnight with the indicated antibodies at 4 °C. For immunoprecipitation with the FLAG epitope, anti-FLAG antibody M2 affinity gel beads (Sigma) were used. The immune complexes were washed three times with 1 ml of lysis buffer, and the antibody-bound proteins were dissolved by boiling in 2× Laemmli sample buffer. After centrifugation, the supernatant proteins were separated by SDS-PAGE and transferred to nitrocellulose membrane (Hybond-C, Amersham Biosciences). The membrane was probed with antibodies, including anti-cyclin T1 and anti-AP-4 (Santa Cruz Biotechnology Inc.), anti-FLAG (Sigma), and anti-Myc (Invitrogen) antibodies; and immunoreactive proteins were visualized by enhanced chemiluminescence (SuperSignal, Pierce). To evaluate the level of OGG1 protein, cells were similarly treated with lysis buffer, and the cell lysate was analyzed by Western blotting using anti-OGG1 antibody (Novus Biologicals, Inc.).

Transfection and Luciferase Assay—Cells were transfected using FuGENE 6 transfection reagent (Roche Applied Science) as described (36). Jurkat cells were transiently transfected by electroporation (42). Briefly, cells (2×10^7/ml) were electroporated in the presence of 2 μg of pcDNA-Tat or control plasmid (pcDNA3.0, Invitrogen) in 400 μl of serum-free RPMI 1640 medium using the Electro Cell Manipulator 600 apparatus (BTX) at 260 V/1050 microfarads. For the internal control, we employed pRL-TK, expressing *Renilla* luciferase, which is not modified by Tat action. The transfected cells were harvested, and the extracts were subjected to luciferase assay using the Luciferase Assay System™ (Promega). The luciferase activity was normalized to *Renilla* luciferase activity as an internal control to assess the transfection efficiency. The data are presented as the -fold increase in luciferase activities (means ± S.D.) relative to the control from three independent transfections.

Reverse Transcription (RT)-PCR—For cDNA synthesis, 1 μg of purified total RNA were reverse-transcribed using oligo(dT) primer and SuperScript II reverse transcriptase. The cDNA was then amplified from each RNA sample with *Taq* PCR Master Mix (Qiagen Inc.) and gene-specific primers designed using Oligo Version 4.0 software (Molecular Biology Insights). The primer sequences for each amplified gene were as follows: *TFPI2* (tissue factor pathway inhibitor-2), 5′-CAG GAG CCA ACA GGA AAT AAC-3′ (forward) and 5′-GAA TAC GAC CCC AAG AAA TGA-3′ (reverse); *OGG1*, 5′-GCG TGC GCA AGT ACT TCC AGC-3′ (forward) and 5′-CCA GTG ATG CGG GCG ATG TTG-3′ (reverse); *OGG1* type 1, 5′-GCG TGC GCA AGT ACT TCC AGC-3′ (forward) and 5′-TAA AGG GAA GAT AAA ACC ATC-3′ (reverse); *OGG1* type 2, 5′-GCG TGC GCA AGT ACT TCC AGC-3′ (forward) and 5′-GCA TCA CAT GAC CAA TTA CTG-3′ (reverse); *MEN1β2* homolog

FLJ23538/clone 137308, 5′-GAG AGG GTT GGT TAG AGA TAC-3′ (forward) and 5′-TGA TTT TAG GTG ATA GTT TCC-3′ (reverse); integrin α7, 5′-AAG ACC GAC AGC AGT TCA AGG-3′ (forward) and 5′-GAC GAA ACC ACG AAA CCA CTA-3′ (reverse); *SLC20A1* (solute carrier family 20, member 1), 5′-TAT GTT TGG TTC TGC TGT GTC-3′ (forward) and 5′-GCT ATC TAT GCT GGT TTC CTC-3′ (reverse); *ENPP2* (ectonucleotide pyrophosphatase/phosphodiesterase-2), 5′-TTC TTT TGG TCT GTG TCA TC-3′ (forward) and 5′-TTC TTC TGT TGT TGG CAT AGT-3′ (reverse); *SEPP1* (selenoprotein P, plasma, 1), 5′-GGA ACA GAG AGC CAG GAC CA-3′ (forward) and 5′-CCT ATG CTG ACC CTT GTG CTT-3′ (reverse); stanniocalcin-1, 5′-AAG AAA GAA AGA GGG AAA AAG-3′ (forward) and 5′-AAC CAA ATC ACA AGG AAA GAA-3′ (reverse); *ETV5* (Ets variant gene-5), 5′-TTG TGT TGT GCC TGA GAG ACT-3′ (forward) and 5′-TCT ATG GGT TTG TGA TTT TTC-3′ (reverse); *NDRG1* (N-Myc downstream regulated gene-1), 5′-GCG GTG GCT GAG AAA ATG TAA-3′ (forward) and 5′-CAA GGT GAT GGG CGG CAG GTA-3′ (reverse); *ARHE* (Ras homolog gene family, member E), 5′-ACT TCG GGT TCT CCT TAC TAT-3′ (forward) and 5′-TTC TCA TCA CTT GGT CTA CAT-3′ (reverse); *HSTF2* (heat shock transcription factor-2), 5′-CAG AAC CAA CCC AAA GTA AGC-3′ (forward) and 5′-ACA GCA TCA ACA GGA AAA CA-3′ (reverse); *NTHL1* (Nth endonuclease III-like 1 (*E. coli*)), 5′-CAG CAG AAG CGA GGA AAA GC-3′ (forward) and 5′-CGC GCA GAG GGC TTG GTT GAG-3′ (reverse); *RGS16* (regulator of G-protein signaling-16), 5′-TGA GAG TCC TGC TGA AAT CCA-3′ (forward) and 5′-CCA ACA ATA ACA AAA ACA ATG-3′ (reverse); hexokinase-2, 5′-GAA CTG GTG GAA GGA GAA GAG-3′ (forward) and 5′-AGG GAA GAA GGA GAG AAA GAG-3′ (reverse); *LTA1* (L-type amino acid transporter subunit-1), 5′-TCG GGG TCT GGT GGA AAA ACA-3′ (forward) and 5′-AAC AAA GGA GGG AAG GGA AAA-3′ (reverse); *SLC1A3* (solute carrier family 1, member 3), 5′-TAT GTT TGG TTC TGC TGT GTG-3′ (forward) and 5′-GCT ATC TAT GCT GGT TTC CTC-3′ (reverse); and β-actin, 5′-CAG CAA GCA GGA GTA TGA CGA-3′ (forward) and 5′-GTG GAC TTG GGA GAG GAC TGG-3′ (reverse). The number of cycles was selected to allow linear amplification of the cDNA under study. PCR products were separated on 1.5% agarose gels and visualized by EtBr staining.

Quantitative real-time RT-PCR was performed essentially as described (39). The oligonucleotide primers and probes for the *OGG1* and β-actin genes were purchased from Applied Biosystems (Assays-on-Demand™). Quantitative measurements of each mRNA level were performed in triplicate. The accuracy of mRNA quantitation for each gene was confirmed by measurement of serially diluted control mRNA samples and comparison of the fluorescent intensity from a standard carve of the mRNA levels. Amplification of β-actin mRNA was performed with all samples to control the variation in mRNA levels. The gene expression levels were normalized to β-actin levels for each mRNA preparation, and the -fold increase in an individual gene was calculated by comparison with the result obtained without PonA stimulation. The non-template control was incubated in each amplification reaction to exclude the contaminating template.

HIV Infection and p24 Determination—PBMCs were stimulated with phytohemagglutinin for 48 h and infected with HIV-1_{MN}. HIV-1_{MN} was challenged at 100 $TCID_{50}$ (where $TCID_{50}$ is the tissue culture infectious dose resulting in 50% infected cells)/2.0–2.5 × 10^6 PBMCs or Jurkat cells for 1 h (43). These cells were washed twice with phosphate-buffered saline (PBS), and HIV-1 p24 antigen concentration in the culture supernatant was measured using a commercial kit (ZeptoMetrix Corp., Buffalo, NY).

mRNA Stability Assay—Total cellular RNA was serially prepared from Tat/293 and mTat/293 cells treated with PonA for 24 h, followed by the treatment with 2 μg/ml actinomycin D (Sigma). The amount of *OGG1* mRNA was analyzed by real-time RT-PCR as described above.

Detection of ROS—The detection of ROS was measured by flow cytometry with a FACScan (BD Biosciences) equipped with argon ion laser delivering 200 megawatts of power at 488 nm, and the results were analyzed using CellQuest™ software (BD Biosciences). After treatment of cells with PonA (10 μM) to induce Tat or mTat, the oxidation-sensitive fluorescent probe 2′,7′-dichlorofluorescein diacetate (Molecular Probes, Inc.) was added to the culture at a final concentration of 5 μM, followed by incubation at 37 °C for 30 min. The cells were washed twice with PBS, resuspended in PBS, and then subjected to the fluorescence-activated cell sorter detection of 5,6-carboxy-2′,7′-dichlorofluorescein (green) at 530 nm.

Measurement of Intracellular Reduced GSH and GSSG Contents—The total cellular GSH and GSSG concentrations were measured using a glutathione quantification kit (Dojindo). Briefly, each cell culture (5 × 10^6 cells) was centrifuged at 2000 × *g* for 5 min, and the cell pellet was resuspended in 100 μl of PBS. The cell suspension was treated with 80 μl of 10 mM HCl, crashed by freeze/thawing repeated twice, and further treated by adding 20 μl of 5% sulfosalicylic acid to precipitate the proteins. The supernatant was obtained by centrifugation at 10,000 × *g* for 10 min, and the total GSH and GSSG concentrations were determined. The sample was incubated with GSH reductase and NADPH at 30 °C for 5 min, and the total GSH concentration thus generated was measured by reaction with 5,5′-dithiobis(2-nitrobenzoic acid) at 30 °C for 10 min. Spectrophotometric detection of 5-mercapto-2-nitrobenzoic acid was performed at 415 nm. The GSSG concentration was determined by performing the same procedure, but GSH was masked by treatment with 2-vinylpyridine and triethanolamine prior to the reaction with GSH reductase and NADPH. The concentration of reduced GSH was determined by subtracting the GSSG concentration from the total GSH concentration. Each determination was performed in triplicate, and experiments were repeated at least twice.

Measurement of Manganese Superoxide Dismutase Activity—The enzymatic activity of manganese superoxide dismutase was measured using a WST-1™ superoxide dismutase assay kit (Dojindo) with slight modifications. Briefly, equal numbers of cells (1.5 × 10^7) were washed twice with PBS, and the cell lysates were extracted by freeze/thawing. The manganese superoxide dismutase activity in the supernatant protein lysate was determined by incubation with WST-1, xanthine, and xanthine oxidase at 37 °C for 20 min. To mask the copper superoxide dismutase and zinc superoxide dismutase activities, the protein lysate was treated with 1 mM KCN. The inhibitory action of manganese superoxide dismutase contained in each cell lysate was assessed by the spectrophotometric determination of WST-1 formazan at 450 nm. Quantitation was achieved by comparison with the absorption of standard manganese superoxide dismutase (Sigma) with known concentrations.

Electrophoretic Mobility Shift Assay—The experimental procedure was carried out as described previously (36). The AP-4 consensus sequence was taken from the 5′-AP-4 site in the *OGG1* promoter. The wild-type and mutant oligonucleotide sequences (sense strand) utilized were as follows: wild-type, 5′-CGG CAG GCA GCA GCT GTG GCG G-3′; and mutant, 5′-CGG CAG GCA GTC GCG ATG GCG G-3′. These oligonucleotides were labeled using a 5′-end labeling kit (Takara) in the presence [γ-^{32}P]dATP (Amersham Biosciences). DNA binding reactions were performed at 4 °C for 20 min in a 10-μl reaction volume. Analysis of binding complexes was performed by electrophoresis on 6% polyacrylamide gels with 0.5 × Tris borate/EDTA buffer, followed by autoradiography. The specificity of DNA binding was assessed by preincubating extracts with anti-AP-4 antibody and competitor at room temperature for 10 min.

Chromatin Immunoprecipitation (ChIP) Assay—ChIP assay was performed according to the recommendations of Upstate Biotechnology, Inc., with some modification. Briefly, cells were cross-linked with 1% formaldehyde for 10 min at room temperature, washed twice with ice-cold PBS, and lysed for 10 min at 2 × 10^6 cells in 200 μl of SDS lysis buffer. The chromatin was sheared by sonication 13 times for 10 s at one-third of the maximum power with 20 s of cooling on ice between each pulse. Cross-linked released chromatin fractions were precleared with salmon sperm DNA and protein A-agarose beads for 1 h, followed by immunoprecipitation overnight with the desired antibodies at 4 °C. The immunoprecipitates were sequentially washed once with lysis buffer, twice with high salt buffer, twice with low salt buffer, and twice with Tris/EDTA buffer. After the wash, immune complexes were collected with salmon sperm DNA and protein A-agarose beads at room temperature for 1 h and extracted with 1% SDS and 0.1 M $NaHCO_3$. The eluted samples were reverse-cross-linked with proteinase K at 65 °C for 6 h and treated with RNase at 37 °C for 1 h. DNA was recovered by phenol/chloroform and chloroform extraction and ethanol precipitation. Finally, DNA was dissolved in 30 μl of Tris/EDTA buffer and subjected to PCR. The primer sequences were as follows: *OGG1* promoter (−615 to −450), 5′-CAA ACG TCC CAT TCC GAG GAA AG-3′ (forward) and 5′-GGC CTT TAG GCG TCC TCT GAG A-3′ (reverse); and β-actin promoter (−980 to −915; used as a control), 5′-TGC ACT GTG CGG CGA AGC-3′ (forward) and 5′-TCG AGC CAT AAA AGG CAA-3′ (reverse). The number of PCR cycles was as follows: 33 PCR cycles for all ChIP experiments and 25 PCR cycles for the input samples, in which PCR amplification was performed under the linear range of AP-4 binding to the *OGG1* promoter. For each reaction, 10% of the cross-linked released chromatin was saved and reversed by proteinase K digestion at 65 °C for 6 h, followed by DNA extraction; and the recovered DNA was used as input control.

Measurement of 8-Oxo-dG—The amounts of 8-oxo-dG in the cellular DNA were measured using a high performance liquid chromatography (HPLC)-electrochemical detector (ECD) system, which is highly selec-

tive, with sensitivity at the femtomole level, as described previously (26, 44). Briefly, cellular DNA was isolated using a DNA extractor WB kit (Wako Pure Chemical Industries, Osaka, Japan). The isolated DNA was digested with P1 nuclease (Wako Pure Chemical Industries) to obtain 8-oxo-dG in the nucleoside form (8-hydroxydeoxyguanosine). The nucleoside solution was filtered with an Ultrafree Probind filter (Millipore Corp.) and injected into an HPLC column (CAPCELL PAK C_{18} MG, Shiseido, Tokyo, Japan) equipped with an ECD (Coulochem II, ESA, Inc.) at a flow rate of 0.8 ml/min with the mobile phase consisting of 10 mM Na_2HPO_4 and 8% methanol. The 8-oxo-dG value in the DNA was calculated as the number of 8-oxo-dG residue/10^6 dG residues.

RNA Interference—siRNA with two thymidine residues (dTdT) at the 3′-end of the sequence was synthesized by Takara. The target sequences were as follows: OGG1 No. 1, 5′-GCC UUC UGG ACA AUC UUU C-3′; OGG1 No. 2, 5′-GCC UUC UGG ACA AUC UUU C-3′; OGG1 No. 3, 5′-GGC UCA GAA AUU CCA AGG U-3′; and green fluorescent protein, 5′-GGC UAC GUC CAG GAG CGC ACC-3′. Transfection of siRNA was performed using Lipofectamine 2000 reagent (Invitrogen). Cells were incubated for 72 h and harvested for the analysis of 8-oxo-dG and OGG1 protein expression.

RESULTS

Establishment and Characterization of Ecdysone-inducible Cell Lines Expressing Tat and mTat—Because Tat is known to impair cell viability and its activity in long-term maintenance of cells expressing Tat may preselect certain cell types and preclude exploration of the Tat-mediated alteration of cellular functions, we adopted a stringent ecdysone-inducible system using PonA, a phytoecdysteroid that is inert in mammals (45). To generate Tat- or mTat-expressing cells upon treatment with PonA, we transfected the pIND-Tat or pIND-mTat plasmid into HEK293-EcR cells stably transfected with pVgRXR expressing the receptor for ecdysone (PonA). These cells were singly isolated by two successive rounds of limiting dilution and screened for expression of Tat proteins and their transcriptional activity in stimulating HIV gene expression.

As shown in Fig. 1*A*, the expression of Tat and mTat proteins was detected after 12 h of PonA treatment and was maintained for at least an additional 60 h. (PonA dose-dependent Tat expression is also shown.) In Fig. 1*B*, Tat-mediated HIV-1 transactivation was examined. As expected, Tat (but not mTat) augmented HIV-1 gene expression in a PonA dose-dependent manner. Fig. 1*C* shows that Tat (but not mTat) bound to endogenous cyclin T1 in cells as reported previously (6–8). These results indicate that both Tat/293 and mTat/293 cells inducibly express Tat proteins and that the functional integrity of Tat is maintained in Tat/293 cells. Thus, we explored the gene expression profile in these cells.

Gene Expression Profile Analysis of Cells Expressing Tat—To identify genes either up-regulated or down-regulated by Tat in the newly established ecdysone-inducible cell lines, the gene expression profiles were compared with and without Tat expression. The mRNA was isolated from Tat/293 and Lac Z/293 cells without (control) and with PonA treatment. The cDNA probes were synthesized from each mRNA, labeled with Cy5 (for Tat- or LacZ-expressing cells) or Cy3 (for non-expressing cells), and hybridized to a gene chip (human 3K DNA CHIP™). Representative results are shown in Fig. 2*A*, where we compared genes expressed in Tat-expressing (Cy5-labeled) and non-expressing control (Cy3-labeled) 293/Tat cells. Similar comparisons were made with LacZ-expressing cells (data not shown).

As shown in Fig. 2*A*, 12 genes, including *TFPI2*, stanniocalcin-1, *SEPP1*, and *OGG1*, were up-regulated by >2-fold by Tat after 24 h of induction upon PonA treatment. Five of these 12 genes were up-regulated by >2-fold even after 12 h of Tat induction. The details of these genes are summarized in Table I. In control LacZ/293 cells, expression of the *TFPI2* gene was up-regulated by 2.0-fold when cells were treated with PonA, suggesting nonspecific stimulation by PonA (data not shown). On the other hand, eight genes were down-regulated to <60% after 24 h of Tat induction (summarized in Table II). Down-regulation of these genes was not observed in LacZ-expressing cells (data not shown).

To confirm these results, we carried out RT-PCR analysis to examine the mRNA levels of Tat-regulated genes before and after Tat induction. We also examined the effect of mTat to further confirm the specificity of Tat action. Fig. 2*B* shows the results of eight genes up-regulated by Tat by >2.3-fold (stanniocalcin-1, *SEPP1*, *OGG1*, *MEN1β2* homolog FLJ23538/clone 137308, *ETV5*, *SLC20A1*, integrin α7, and *ENPP2*; excluding *TFPI2*). Among these genes, stanniocalcin-1, *SEPP1*, and *ETV5* were also up-regulated by induction of mTat or even LacZ, suggesting a nonspecific effect of PonA. Thus, we concluded that five genes (*OGG1*, *MEN1β2* homolog FLJ23538/clone 137308, integrin α7, *SLC20A1*, and *ENPP2*) are specifically up-regulated by Tat because these genes were not up-regulated by either mTat or LacZ. Whereas *ENPP2* was up-regulated after 12–24 h of Tat induction and subsequently down-regulated, the other four genes were constitutively up-regulated.

Similarly, RT-PCR analysis was performed with the eight genes down-regulated by Tat (Fig. 2*C*). Two of the genes (*SLC1A3* and *LTA1*) were down-regulated by mTat or LacZ. The other six genes were down-regulated by Tat, but not by mTat or LacZ. Among the genes down-regulated by Tat, *NDRG1*, *RGS16*, and hexokinase-2 are known to be under the transcriptional control of p53 (46–48), an observation consistent with previous reports of Tat down-regulating the action of p53 (49, 50).

Induction of OGG1 Gene Expression by Tat—Because Tat up-regulated the *OGG1* gene the most, we further analyzed the effect of Tat on *OGG1* mRNA expression and stability. The human *OGG1* gene encodes two isoforms, type 1 (a and b) and type 2 (a, b, and c), resulting from alternative splicing of the single *OGG1* precursor mRNA (51). As shown in Fig. 3*A*, Tat induced all types of *OGG1* mRNA. We carried out real-time RT-PCR to determine more precisely the mRNA levels of *OGG1* before and after Tat induction. As shown in Fig. 3*B*, *OGG1* gene expression was up-regulated by 3.6-, 6.7-, 9.8-, and 8.2-fold upon Tat expression after 6, 12, 24, and 48 h of PonA treatment, respectively. mTat did not affect *OGG1* gene expression (Fig. 3*B*). A similar extent of stimulation was observed for OGG1 protein levels as revealed by Western blotting (Fig. 3*C*). No induction of OGG1 protein was observed when mTat was induced. Induction of OGG1 protein by Tat (but not mTat) was confirmed in Jurkat T cells, a natural host of HIV-1 infection (Fig. 3*C*, *right panels*). Furthermore, the effect of HIV-1 infection on *OGG1* gene expression was examined with PBMCs isolated from two individuals and Jurkat cells. These cells were infected with $HIV\text{-}1_{MN}$, and the *OGG1* mRNA level was quantified by real-time RT-PCR together with the amounts of HIV-1 produced in the culture supernatant. As shown in Fig. 3*D*, up-regulation of *OGG1* mRNA levels upon HIV-1 infection was observed and was associated with elevation of viral p24 antigen levels. Mock infection did not induce *OGG1* expression (data not shown).

Furthermore, we examined the effect of Tat on the stability of *OGG1* mRNA using PonA-inducible cells. After 24 h of Tat or mTat induction, cells were treated with actinomycin D, and total RNA samples were obtained after 1, 3, 5, and 7 h of actinomycin D treatment to determine the level of *OGG1* mRNA. As shown in Fig. 3*E*, the decay profiles of *OGG1* mRNA were similar in cells expressing Tat and mTat (control), with half-lives of 5.0 and 4.3 h, respectively. These findings indicate that the positive effects of Tat on *OGG1* gene expression are at the level of transcription.

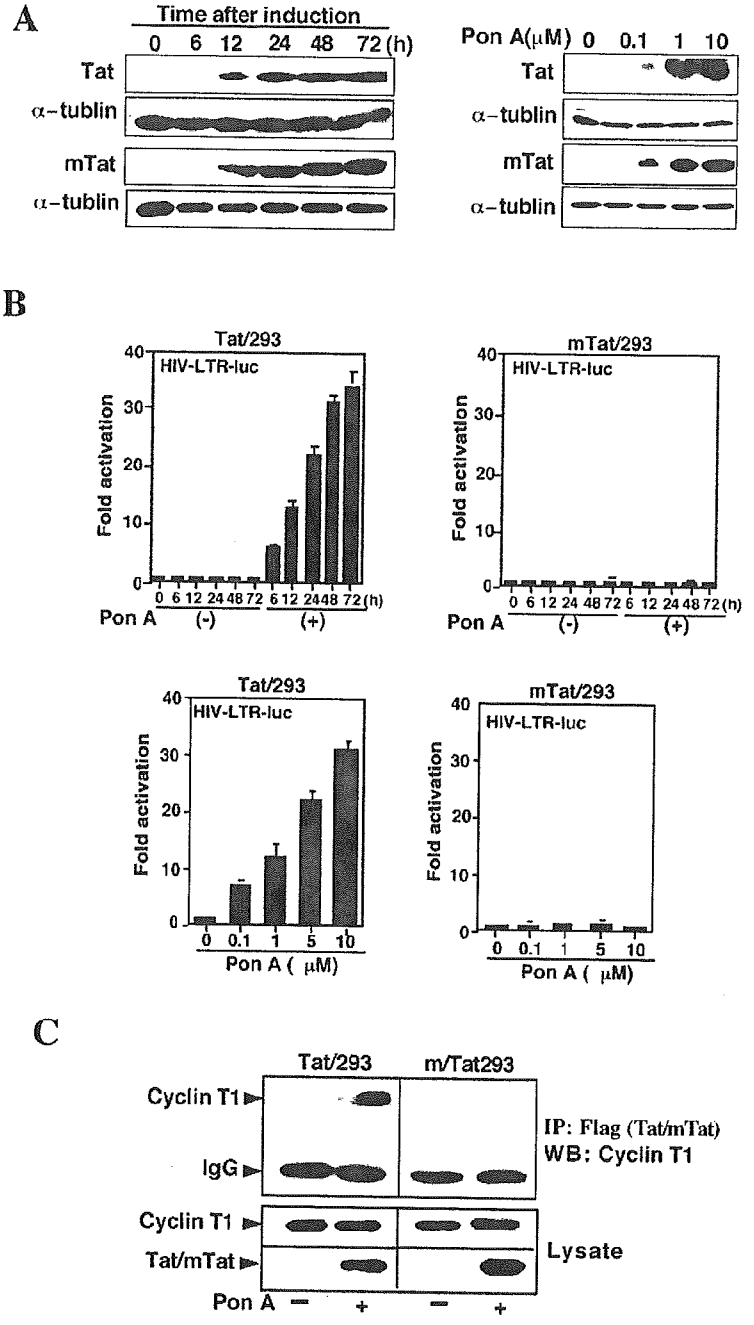

FIG. 1. **Ecdysone-inducible cell lines expressing Tat and mTat.** *A*, inducible expression of Tat and mTat. Tat/293 and mTat/293 cells were treated with PonA (10 μM) for the indicated periods of time (*left panels*) at the indicated concentrations (*right panels*). The FLAG-tagged Tat and mTat proteins were detected by Western blotting with anti-FLAG antibody. Anti-α-tubulin antibody was used to indicate that the equivalent amount of protein from each cell lysate was loaded. *B*, Tat-mediated transactivation of HIV-1 gene expression. Tat/293 (*left panels*) and mTat/293 (*right panels*) cells were transfected with HIV-1 long terminal repeat (*LTR*)-luciferase (*luc*), maintained in culture for 24 h, and then treated for the indicated periods of time with 10 μM PonA (*upper panels*) or for 48 h with various concentrations of PonA (*lower panels*). *C*, co-immunoprecipitation of cyclin T1 with Tat. Tat/293 and mTat/293 cells were treated with PonA for 24 h, and the cell lysates were immunoprecipitated (*IP*) with anti-FLAG antibody (detecting Tat). Immune complexes were collected and subjected to SDS-PAGE, followed by Western blotting (*WB*) with anti-cyclin T1 antibody. One-tenth of each protein lysate used in each reaction was loaded as the input control.

Induction of OGG1 Expression Is Not through the Oxidative Stress Induced by Tat—Because Tat is known to induce oxidative stress (12, 15, 17), it is possible that *OGG1* induction might be an indirect effect of Tat, although it is not yet known whether oxidative stress induces *OGG1* gene expression. We first examined whether Tat induces oxidative stress in Tat/293 cells. Fluorescence-activated cell sorter analysis with the oxidation-sensitive fluorescent probe 2′,7′-dichlorofluorescein diacetate showed that Tat (but not mTat) increased the intracellular ROS levels (Fig. 4*A*). We measured the intracellular levels of GSH and GSSG. As expected, the content of GSSG, the oxidized form of GSH, was increased (~2.3-fold) in Tat-expressing cells in contrast to control mTat-expressing cells (Fig. 4*B*). The GSH (reduced form) level in Tat-expressing cells was decreased to 57% of that in control cells. No significant reduction in GSH was detected in mTat-expressing cells. Furthermore, the manganese superoxide dismutase activity was down-regulated by Tat as reported previously (12). After 24 h of Tat induction, the manganese superoxide dismutase activity was decreased to 59% (Fig. 4*C*).

These results led us to examine whether Tat-induced *OGG1* gene expression is attributable to the oxidative stress associated with Tat action. However, treatment with antioxidants did not block Tat-mediated *OGG1* induction (Fig. 4*D*). 293/Tat cells were pretreated with antioxidants, including pyrrolidine dithiocarbamate, *N*-acetyl-L-cysteine, epigallocatechin gallate (a phenolic antioxidant), and Trolox (a water-soluble vitamin E analog), prior to Tat induction (Fig. 4*D*, *left panel*). When the *OGG1* mRNA was measured by real-time RT-PCR, Tat-induced *OGG1* expression was not affected by the antioxidants. In

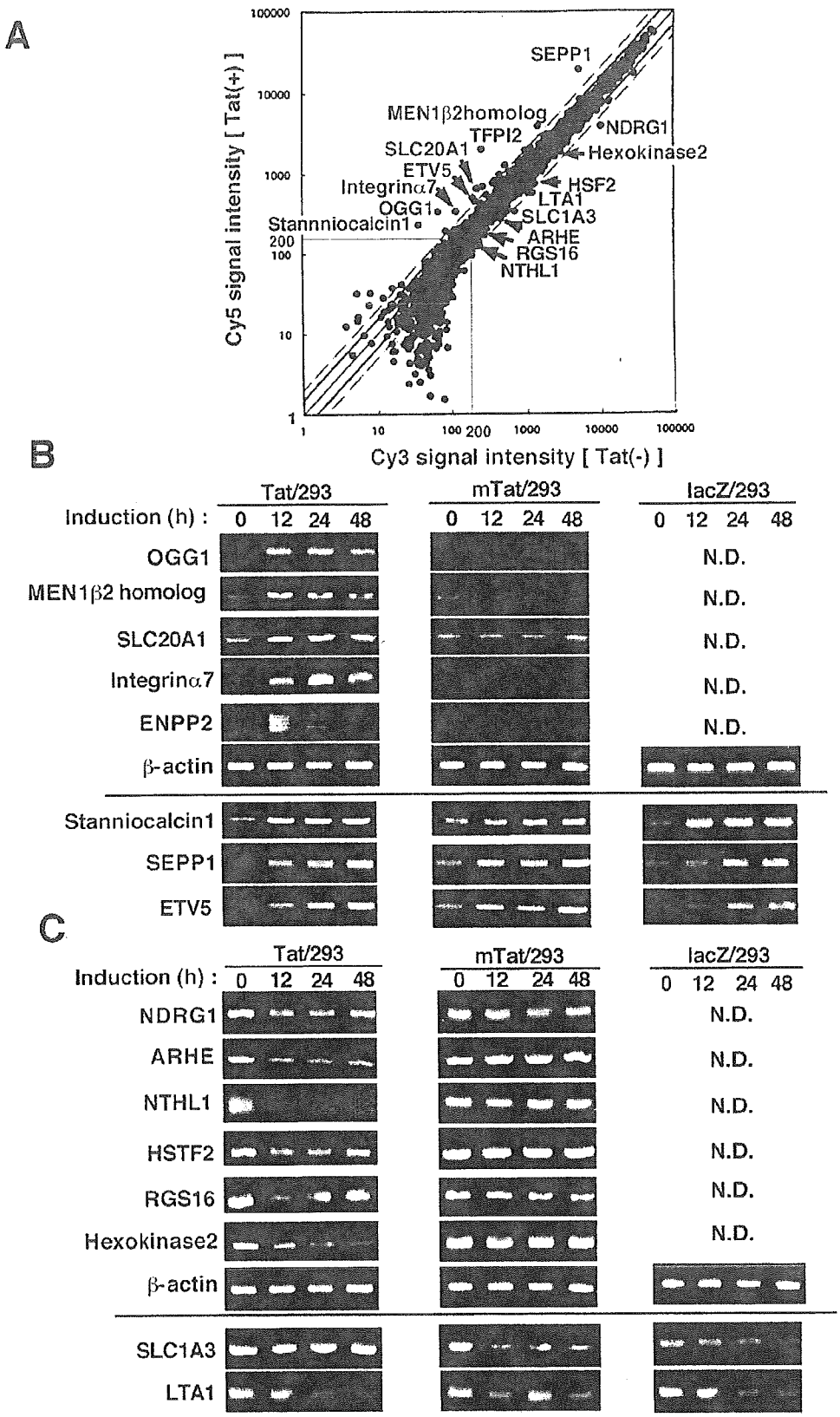

FIG. 2. **Gene expression profile analysis and confirmatory RT-PCR.** *A*, scatter plot of the hybridization signal intensity of genes in cells expressing Tat *versus* control cells. The mRNA was isolated from Tat/293 cells without (control) or with PonA treatment for 24 h. The cDNA probes were synthesized from the mRNA of each cell culture and labeled with either Cy5 (for Tat-expressing cells) or Cy3 (for control 293 cells). These probes were hybridized, in combination, to a gene chip (human 3K DNA CHIP™). The signal intensity of each gene on the microarray chip was

TABLE I
Genes up-regulated by Tat

Gene	Induction		GenBank™ accession no.
	12 h	24 h	
	-fold		
TFPI2[a]	6.5[b]	7.9 ± 0.7[c]	NM_006528
Stanniocalcin-1[a]	2.4	4.0 ± 0.3	NM_003155
SEPP1[a]	2.4	3.4 ± 0.3	NM_005410
OGG1	2.6	2.7 ± 0.2	NM_016819
Human clone 137308 mRNA; similar to *MEN1*β_2[d]	1.1	2.7 ± 0.2	U60873
ETV5 (Ets-related molecule)[a]	1.8	2.6 ± 0.2	NM_004454
Homo sapiens cDNA, similar to *MEN1*β_2[d]	1.1	2.5 ± 0.2	AK027191
SLC20A1	1.8	2.5 ± 0.3	NM_005415
Integrin α7	1.9	2.4 ± 0.1	NM_002206
ENPP2/autotaxin	1.7	2.3 ± 0.2	NM_006209
ABCG1 (ATP-binding cassette, subfamily G (WHITE), member 1)	1.3	2.1 ± 0.1	NM_004915
Calcium-binding protein p22	2.1	2.0 ± 0.1	BC001646
Laminin α3	1.4	2.0 ± 0.1	NM_000227

[a] Nonspecifically up-regulated by PonA treatment (see Fig. 2 for the results of RT-PCR).
[b] Data from single determinations 12 h after Tat induction.
[c] Data from triplicate determinations 24 h after Tat induction (expressed as means ± S.D.).
[d] Different cDNA segments of the same gene.

TABLE II
Genes down-regulated by Tat

Gene	Induction		GenBank™ accession no.
	12 h	24 h	
	-fold		
NDRG1	0.5[a]	0.4 ± 0.1[b]	NM_006096
ARHE	0.5	0.5 ± 0.1	NM_005168
SLC1A3[c]	0.7	0.5 ± 0.1	NM_004172
NTHL1	0.8	0.6 ± 0.1	NM_002528
HSTF2	0.5	0.6 ± 0.1	NM_004506
RGS16	0.7	0.6 ± 0.1	NM_002928
Hexokinase-2	0.7	0.6 ± 0.1	NM_000189
LTA1[c]	1.3	0.6 ± 0.2	AF104032

[a] Data from single determinations 12 h after Tat induction.
[b] Data from triplicate determinations 24 h after Tat induction (expressed as means ± S.D.).
[c] Nonspecifically up-regulated by PonA treatment (see Fig. 2 for the results of RT-PCR).

addition, H_2O_2 and oxidative stress inducers such as inflammatory cytokines (tumor necrosis factor-α and interleukin-1β) and lipopolysaccharide could not up-regulate *OGG1* gene expression (Fig. 4*D*, *right panel*). In support of these findings, when we performed transient luciferase assay using the *OGG1* promoter construct, no *OGG1* induction by these stimuli was observed (data not shown), consistent with a previous report by Dhénaut *et al.* (37). Therefore, it is unlikely that Tat induces *OGG1* expression through ROS production.

Transactivation of OGG1 by Tat—These observations prompted us to examine the possibility that Tat-mediated *OGG1* expression is the direct effect of Tat. We thus examined the effect of Tat on *OGG1* promoter activity. The transient luciferase assay was performed on various regions of the *OGG1* promoter linked to the luciferase reporter gene (Fig. 5). As shown in Fig. 5*A*, Tat stimulated the transcriptional activity of the reporter constructs containing the sequence upstream from position −472. Whereas the sequence upstream from position −945 was dispensable for Tat-mediated transactivation, no such effect was observed when the region spanning positions −945 to −472 was deleted (Fig. 5*A*, *lower left panel*). In 293 cells expressing mTat, no induction of *OGG1* promoter activity (other than the constitutive transcriptional activity) was observed. We also examined the Tat-mediated transactivation of the *OGG1* promoter in Jurkat cells and obtained essentially the same results (Fig. 5*A*, *lower right panel*).

Thus, Tat appears to transactivate *OGG1* expression through transcription factors located within the *OGG1* promoter region from positions −945 to −472. To further elucidate the mechanism by which Tat induces *OGG1* transcription, we created specific mutants lacking binding sites for GATA, AP-4, and/or AP-2 located in this region. When AP-4 sites were mutated, Tat no longer augmented the promoter activity (Fig. 5*B*, *black bars*). However, no reduction in Tat-mediated transactivation was observed when other sites were mutated. In addition, the basal promoter activity was augmented when the 5′-AP-4 site was mutated, whereas mutation of the GATA, AP-2, and 3′-AP-4 sites had little effect on the basal *OGG1* promoter activity (Fig. 5*B*, *hatched bars*), indicating that AP-4 acts as a transcriptional repressor of *OGG1* expression. These results suggest that AP-4 sites are required for Tat-induced *OGG1* gene expression and that the 5′-AP-4 site negatively regulates *OGG1* gene expression. In fact, overexpression of AP-4 inhibited both the Tat-stimulated and basal levels of *OGG1* gene expression without affecting the level of Tat expression (Fig. 5*C*).

Tat Interacts with AP-4 and Removes It from the OGG1 Promoter—To further investigate the mechanism by which Tat stimulates *OGG1* gene expression, we first examined the effect of Tat on AP-4 DNA binding by electrophoretic mobility shift assay. As shown in Fig. 6*A*, constitutive AP-4 DNA binding was observed in the cells, and a significant reduction in AP-4 DNA binding was observed when Tat was induced by PonA treatment. No such effect was observed when mTat was expressed. We then examined whether Tat associates with AP-4 in cultured cells by co-immunoprecipitation with either Tat (FLAG epitope-tagged) or AP-4 (Myc epitope-tagged). As shown in Fig. 6*B*, when Tat was immunoprecipitated with anti-FLAG antibody, endogenous AP-4 protein was detected within the immune complex. No AP-4 was co-immunoprecipitated with mTat. Conversely, when AP-4 was immunoprecipitated with

plotted. Genes with a signal intensity <200 U (of Cy5 and Cy3) were excluded from further analysis. *Solid* and *dashed lines* indicate the upper and lower boundaries of 1.5- and 2.0-fold changes, respectively. *B* and *C*, confirmation of genes up- or down-regulated by Tat using RT-PCR. *B*, genes up-regulated by Tat. Up-regulation of the stanniocalcin-1, *SEPP1*, and *ETV5* genes observed in cDNA array analysis appeared to be unspecific. *C*, genes down-regulated by Tat. Down-regulation of the *SLC1A3* and *LTA1* genes was considered nonspecific. RT-PCR analysis was performed with gene-specific primers and total RNA prepared from Tat/293, mTat/293, and LacZ/293 cells. Each cell culture was treated with PonA (10 μM) for the indicated periods of time. *N.D.*, not determined.

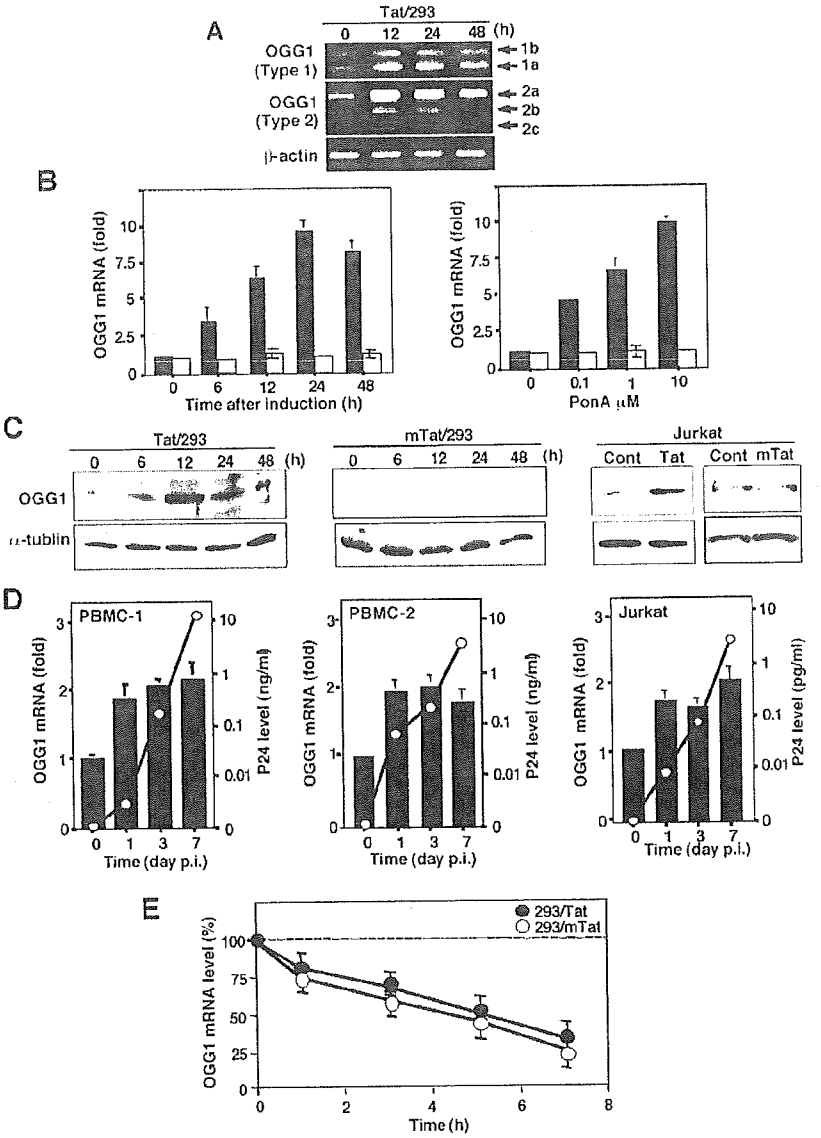

FIG. 3. **Induction of OGG1 by Tat.** *A*, induction of *OGG1* mRNA species by Tat. Tat/293 cells were treated with PonA (10 μM) for the indicated periods of time. RT-PCR analysis was performed with specific primers for the *OGG1* type 1 and 2 genes. Note that all of the splicing variants of *OGG1* mRNA were similarly up-regulated by Tat. *B*, quantitation of *OGG1* mRNA induction by real-time RT-PCR analysis. Tat/293 (*black bars*) and mTat/293 (*white bars*) cells were treated with 10 μM PonA for the indicated periods of time (*left panel*) or for 24 h with various concentrations of PonA (*right panel*). The total RNA was purified from each culture preparation and subjected to real-time RT-PCR using an *OGG1* primer/probe mixture. *C*, induction of OGG1 protein by Tat. Tat/293 (*left panel*) and mTat/293 (*middle panel*) cells were treated with PonA (10 μM) for the indicated periods of time, and OGG1 proteins were examined by Western blotting with anti-OGG1 antibody. Jurkat cells (*right panel*) were transfected with pcDNA-Tat, pcDNA-mTat, or the control (*Cont*) plasmid for 24 h. *D*, induction of *OGG1* mRNA by HIV-1 infection. PBMCs from two individuals and Jurkat cells were infected with HIV-1_{MN} at 100 $TCID_{50}$, and the *OGG1* RNA levels were measured by real-time RT-PCR. HIV-1 production was measured by the viral p24 antigen level in the culture supernatants. *p.i.*, post-infection in days. *E*, effect of Tat on *OGG1* mRNA stability. Tat/293 and mTat/293 cells were treated with PonA (10 μM) for 24 h and treated with actinomycin D (2 μg/ml). Total cellular RNA was obtained at the indicated time points, and the amount of *OGG1* mRNA was determined by real-time RT-PCR analysis. The experiments were performed in triplicate.

anti-Myc antibody, Tat (but not mTat) was co-immunoprecipitated (Fig. 6*B*, *lower panels*).

Furthermore, the ChIP assay was performed to examine whether the inhibition of AP-4 DNA binding by Tat occurs at the endogenous *OGG1* gene promoter. Tat/293 and mTat/293 cells were transfected with plasmids expressing Myc-tagged AP-4 or Myc-tagged LacZ (control), stimulated with PonA to express Tat or mTat, treated with formamide, and sonicated, and the cross-linked protein·DNA complex was immunoprecipitated with specific antibodies recognizing the Myc (AP-4) or V5 (Tat) epitope. The immunoprecipitated DNA was analyzed by PCR using primer pairs for the AP-4-binding sites within the *OGG1* promoter (−615 to −450). As demonstrated in Fig. 6*C*, a significant reduction in AP-4 bound to the *OGG1* promoter DNA was observed, and the extent of reduction was proportionate to the amount of Tat expressed (corresponding to the time-dependent expression of Tat in Fig. 1). No such effect was observed when mTat was expressed. The antibody to Tat precipitated the *OGG1* promoter (Fig. 6*C*, *left panels*), indicating that the Tat·AP-4·DNA ternary complex may be transiently formed. These observations indicate that Tat directly activates *OGG1* gene expression through sequestrating AP-4, a negative transcriptional regulator of *OGG1* expression.

Reduction of 8-Oxo-dG Levels by Tat and Effect of OGG1 Knockdown—Because OGG1 is responsible for the excision/repair of the oxidation-damaged DNA by excising 8-oxo-dG (30) and because Tat induces expression of OGG1, we measured the amounts of 8-oxo-dG in the cellular DNA by the HPLC-ECD method (26). Fig. 7*A* shows the levels of 8-oxo-dG before and after Tat expression. In control cells, the level of 8-oxo-dG was 8.7 ± 0.34 residues/10^6 dG residues (Fig. 7*B*). However, upon expression of Tat, the 8-oxo-dG levels were reduced to 7.7 ± 1.6 (0.89-fold), 5.6 ± 0.30 (0.64-fold), and 4.5 ± 1.2 (0.52-fold) residues/10^6 dG residues after 6, 12, and 24 h of Tat induction, respectively. Statistically significant reduction was observed after 12 and 24 h of Tat induction. No significant reduction in 8-oxo-dG levels was observed when mTat was expressed. Taken together, these observations indicate that Tat prevents accumulation of 8-oxo-dG by directly up-regulating OGG1 expression.

To confirm these findings, we adopted a siRNA technique to specifically knock down *OGG1* mRNA and examined the effect of Tat on the level of 8-oxo-dG when endogenous OGG1 was

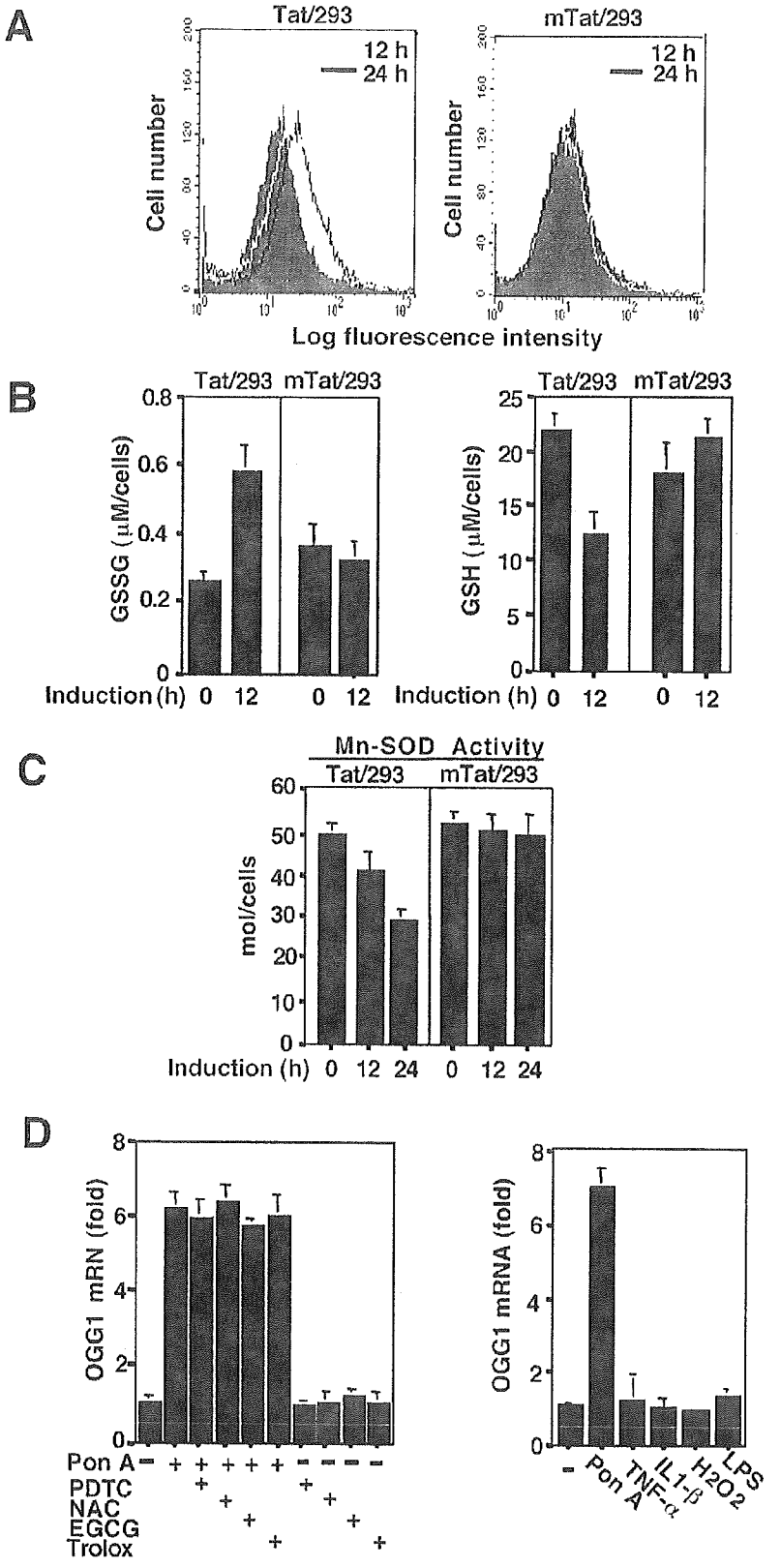

FIG. 4. **Induction of oxidative stress by Tat and effects of antioxidants on Tat-mediated *OGG1* expression.** *A*, accumulation of ROS by Tat. Tat/293 (*left panel*) and mTat/293 (*right panel*) cells were treated with 5 μM 2′,7′-dichlorofluorescein diacetate for 30 min, followed by treatment with PonA (10 μM) for 12 or 24 h. The intracellular 5,6-carboxy-2′,7′-dichlorofluorescein level (the indicator for ROS) in the cells was measured by flow cytometry. *B*, changes in GSSG (*left panel*) and GSH (*right panel*) contents by Tat. Tat/293 and mTat/293 cells were treated with PonA at 10 μM for 12 h, and GSH and GSSG contents were determined by the 5,5′-dithiobis(2-nitrobenzoic acid)/GSH reductase recycling method. To measure the GSSG content, GSH was masked by treatment with 2-vinylpyridine and triethanolamine prior to the reaction with GSH reductase and NADPH. *C*, inhibition of manganese superoxide dismutase (*Mn-SOD*) activity by Tat. Tat/293 and mTat/293 cells were treated with PonA (10 μM) for 12 or 24 h. The lysates were treated with KCN to mask copper superoxide dismutase and zinc superoxide dismutase activities, and then the manganese superoxide dismutase activity was measured by enzymatic assay. *D*, effects of various antioxidants on Tat-induced *OGG1* expression. Total RNA was prepared from each cell culture, and *OGG1* mRNA was quantitated by real-time RT-PCR as described in the legend to Fig. 2*B*. *Left panel*, Tat/293 cells were pretreated for 1 h with pyrrolidine dithiocarbamate (*PDTC*; 100 μM), *N*-acetyl-L-cysteine (*NAC*; 20 mM), epigallocatechin gallate (*EGCG*; 20 μM), or Trolox (100 μM) and stimulated with PonA (10 μM) for 12 h, and total RNA was prepared. *Right panel*, Tat/293 cells were treated with tumor necrosis factor-α (*TNF-α*; 5 ng/ml), interleukin-1β (*IL-1β*; 10 ng/ml), H_2O_2 (1 mM), lipopolysaccharide (*LPS*; 200 ng/ml), or PonA (10 μM) for 12 h, and the *OGG1* RNA levels were measured.

depleted. We synthesized three kinds of 21-nucleotide siRNA duplexes corresponding to the conserved *OGG1* mRNA regions utilized in all types of *OGG1* mRNA species. Cells transduced with OGG1 siRNA (No. 1) showed the greatest reduction in OGG1 protein levels compared with the control (Fig. 7*C*) and were thus used in the following experiment. As demonstrated

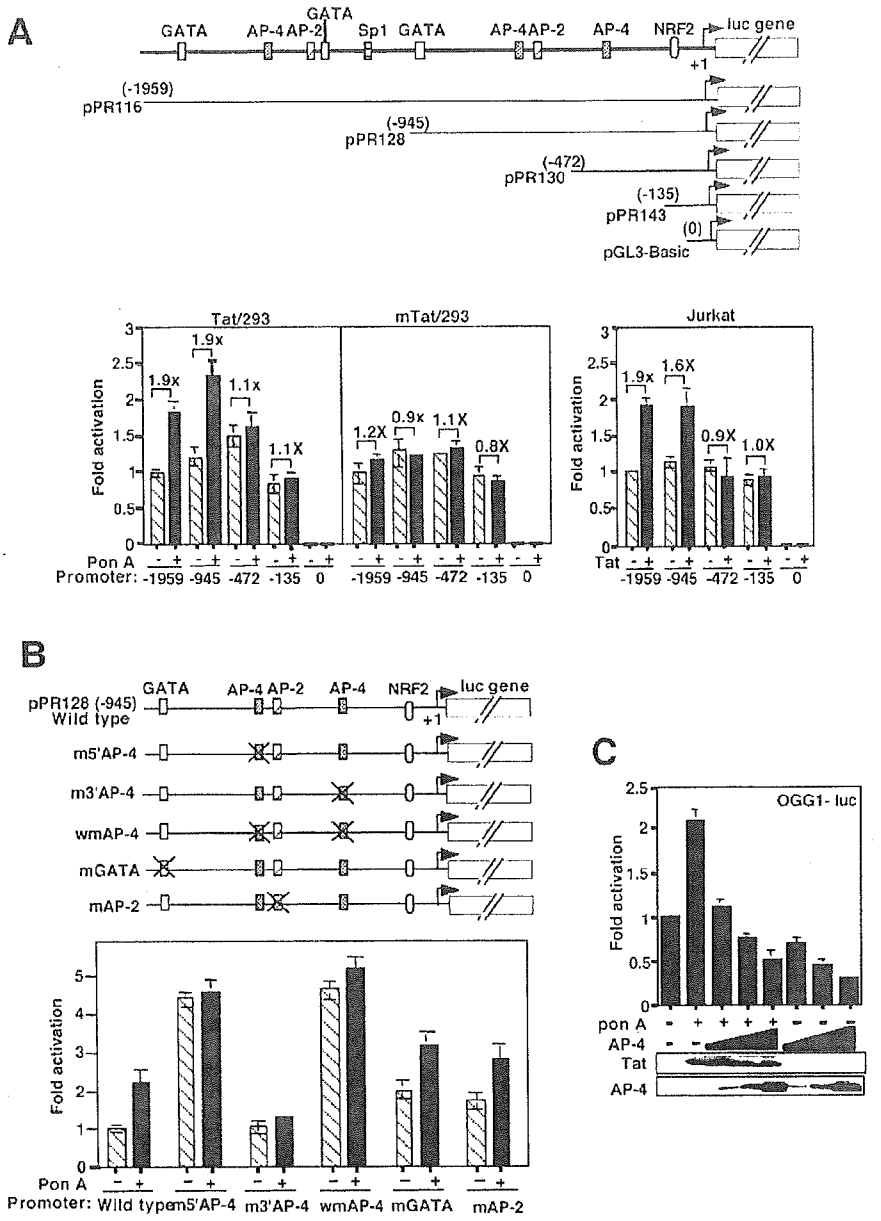

FIG. 5. **Tat directly activates *OGG1* gene expression.** *A*, effect of Tat on *OGG1* promoter activity. Schematic diagrams of the *OGG1* promoter constructs are shown, indicating the positions of various *cis*-elements for transcription factors GATA, AP-4, AP-2, Sp1, and NRF2 (nuclear factor erythroid-related factor 2) (*upper panel*). Tat/293 and mTat/293 cells (*lower left panel*) were transfected with various *OGG1* promoter constructs, incubated for 24 h, and treated (*black bars*) or not (*hatched bars*) with PonA (10 μM) for an additional 24 h. Jurkat cells (*lower right panel*) were transfected with *OGG1* promoter constructs in the presence (*black bars*) or absence (*hatched bars*) of pcDNA-Tat. Cells were harvested, and the luciferase (*luc*) activity was measured. The data are presented as the -fold increase in luciferase activity (means ± S.D.) relative to the transcriptional activity of the full-length *OGG1* promoter (pPR116) from three independent experiments. *B*, involvement of AP-4 in Tat-mediated *OGG1* expression. Various mutations in the binding sites for GATA, AP-4, and AP-2 were introduced into a wild-type *OGG1* promoter (pPR128-luc), and the effects of Tat were examined. Schematic representations of wild-type and mutant pPR128-luc constructs are shown (*upper panel*). Tat/293 cells were transfected with these reporter constructs, and the effects of Tat were similarly examined (*lower panel*). Note the increase in basal promoter levels with mutants containing a substitution in the 5′-AP-4 site and the lack of Tat response in mutants containing 5′- and/or 3′-AP-4 sites. *C*, repression of *OGG1* expression by AP-4. Tat/293 cells were transfected with pPR116-luc together with various amounts of plasmid expressing Myc-AP-4, incubated for 24 h, and treated with PonA (10 μM) for an additional 24 h to induce Tat expression (*upper panel*). The dose-dependent expression of AP-4 was revealed by Western blotting with anti-Myc tag antibody (*lower panels*). Tat protein expression was monitored using anti-FLAG antibody.

in Fig. 7*D*, OGG1 depletion by OGG1 siRNA (No. 1) resulted in a significant increase in the level of 8-oxo-dG (1.6-fold with the control and 1.4-fold with control siRNA). More important, 8-oxo-dG formation was induced by Tat when OGG1 was depleted (2.2-fold with the control and 1.9-fold with control siRNA). In addition, overexpression of AP-4, acting as a negative regulator of *OGG1* expression, increased the level of 8-oxo-dG (1.8-fold with the control).

DISCUSSION

In this study, we have explored the biological effects of Tat using gene expression profile analysis. We found that (i) Tat induces the *OGG1* gene and that (ii) Tat down-regulates the *NDRG1*, *RSG16*, and hexokinase-2 genes. The latter genes are known to be under the transcriptional control of p53 (46–48). Interestingly, Li *et al.* (49) observed the repression of p53 mRNA by Tat. Moreover, Tat was shown to directly inactivate p53 by protein-protein interaction (50, 52). Thus, the Tat-mediated down-regulation of these genes is consistent with previous findings. However, Tat-mediated OGG1 induction has not been reported. Thus, in this study, we analyzed the mechanism by which Tat induces *OGG1* gene expression.

We found that Tat-mediated OGG1 induction is not through stabilization of the *OGG1* mRNA. In addition, Tat-mediated *OGG1* induction was not reversed by treatment with antioxidants, indicating that Tat-mediated *OGG1* induction could not be attributable to oxidative stress induced by Tat. By performing transient luciferase assay using the reporter plasmid containing various regions of *OGG1*, we found that Tat induces *OGG1* gene expression through the central AP-4 site (located at positions −545 to −540) in its upstream region. Although AP-4 is known to activate expression of the SV40 (53) and transforming growth factor-β (54) genes, it is also known to repress expression of the human angiotensinogen (55) and HIV-1 (56) genes, although the mechanism of AP-4 action has not been clarified. Our experiments have revealed that AP-4 negatively regulates *OGG1* gene expression via binding to the central

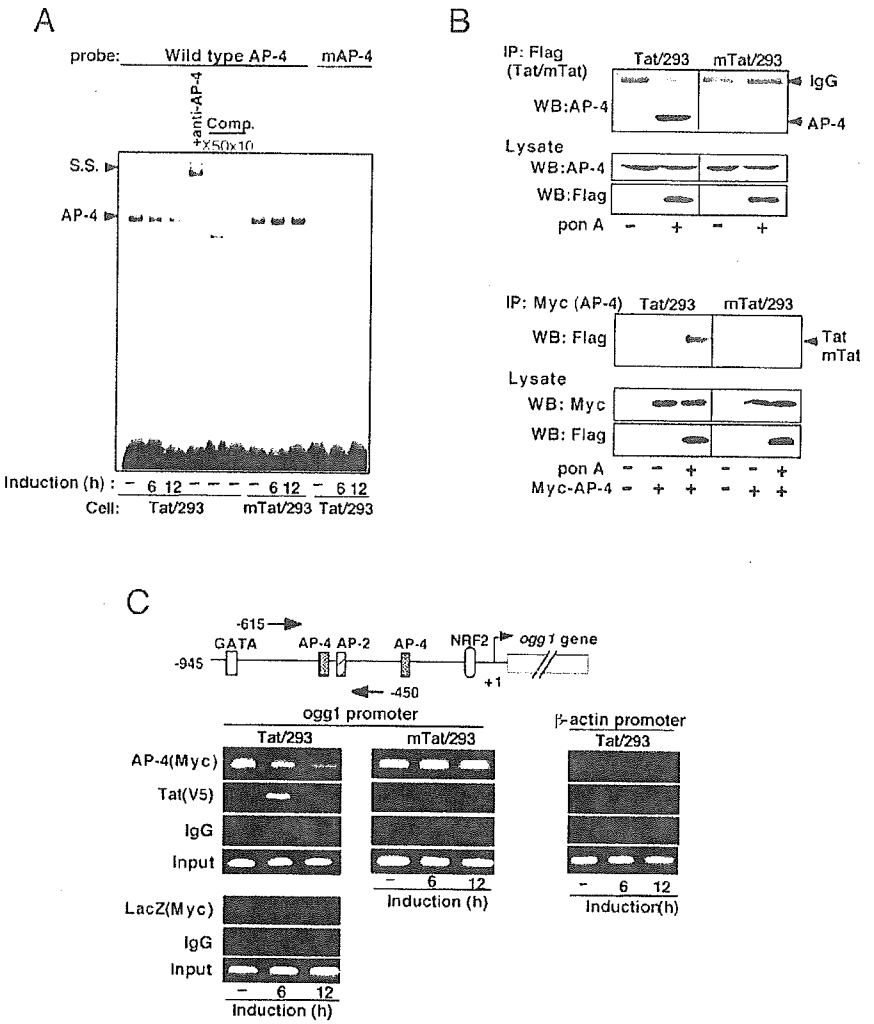

FIG. 6. **Mechanism by which Tat induces *OGG1* gene expression: Tat interacts with AP-4 and removes AP-4 from the *OGG1* promoter.** *A*, effect of Tat on AP-4 DNA binding. Nuclear extracts were prepared from Tat/293 and mTat/293 cells, and AP-4 DNA binding was examined by electrophoretic mobility shift assay using AP-4 or mutant AP-4 probes. To verify the AP-4·DNA complex, nuclear extracts were incubated with anti-AP-4 antibody or excess amounts of competitor oligonucleotides (10- or 50-fold). The positions of the specific protein·DNA and supershifted (*S.S.*) complexes (*arrowheads*) are indicated. *B*, interaction between Tat and AP-4 *in vivo*. *Upper panel*, cell lysates were prepared, and immune complexes containing Tat or mTat were immunoprecipitated (*IP*) with anti-FLAG antibody (detecting Tat). The immunoprecipitates were separated by SDS-PAGE, followed by Western blotting (*WB*) with anti-AP-4 antibody. One-tenth of each protein lysate used in each reaction was loaded as the input control. *Lower panels*, Tat/293 and mTat/293 cells were transfected with plasmid expressing Myc-AP-4, and expression of Tat proteins was induced by PonA (10 μM). The cell lysates were immunoprecipitated with anti-Myc antibody (detecting AP-4), and the immune complex was analyzed for the presence of Tat by Western blotting with anti-FLAG antibody. *C*, ChIP assay. *Upper panel*, the *OGG1* promoter region amplified by the primer pairs in ChIP assay is illustrated. *Arrows* indicate the positions of PCR primers. *Lower panels*, cell lysates were prepared from Tat/293 and mTat/293 cells that were transfected with plasmid expressing Myc-AP-4 or Myc-LacZ (control) and treated with PonA (10 μM) for expression of Tat and mTat. Cross-linked chromatin fragments were prepared, and the association of AP-4, LacZ, Tat, and *OGG1* promoter DNA was analyzed by ChIP assay. The recovered DNA was amplified by PCR with promoter-specific primers and analyzed on a 2% agarose gel. DNAs isolated from sonicated cross-linked chromatin fragments were used as inputs. The β-actin promoter DNA was similarly analyzed as a control.

AP-4 site and that Tat activates *OGG1* promoter activity by sequestrating AP-4 from the *OGG1* promoter. Thus, the positive effect of Tat on *OGG1* gene expression appears to be a direct effect.

Intriguingly, we observed that the extent of oxidation-induced guanosine modification (8-oxo-dG) was reduced, although Tat induced oxidative stress as revealed by the increase in ROS and GSSG and the decrease in manganese superoxide dismutase activity. When OGG1 expression was knocked down by siRNA, the amount of 8-oxo-dG was increased, suggesting that the Tat-induced reduction of 8-oxo-dG requires *OGG1* gene expression and that the Tat-mediated induction of OGG1 appears to be independent of Tat pro-oxidant action.

Thus, in addition to its crucial role in viral replication, Tat appears to play a role in maintenance of the genetic integrity of proviral and host cell DNAs. Although various conditions associated with HIV infection and replication are pro-oxidant (12, 13, 57–59), the observed mutations accumulated within the HIV genome have been revealed to be in favor of the G:C to A:T transition (18–22) rather than the G:C to T:A transversion mediated by the oxidative modification. This is in contrast with most of the mutations associated with human cancers, where the G:C to T:A transversion is predominant (28, 29). If induction of OGG1 were through oxidative stress associated with Tat actions, the level of 8-oxo-dG should have been higher in Tat-expressing cells than in control cells. These findings indicate that Tat-mediated OGG1 induction is more than a feedback action. Although additional studies are needed, such as the

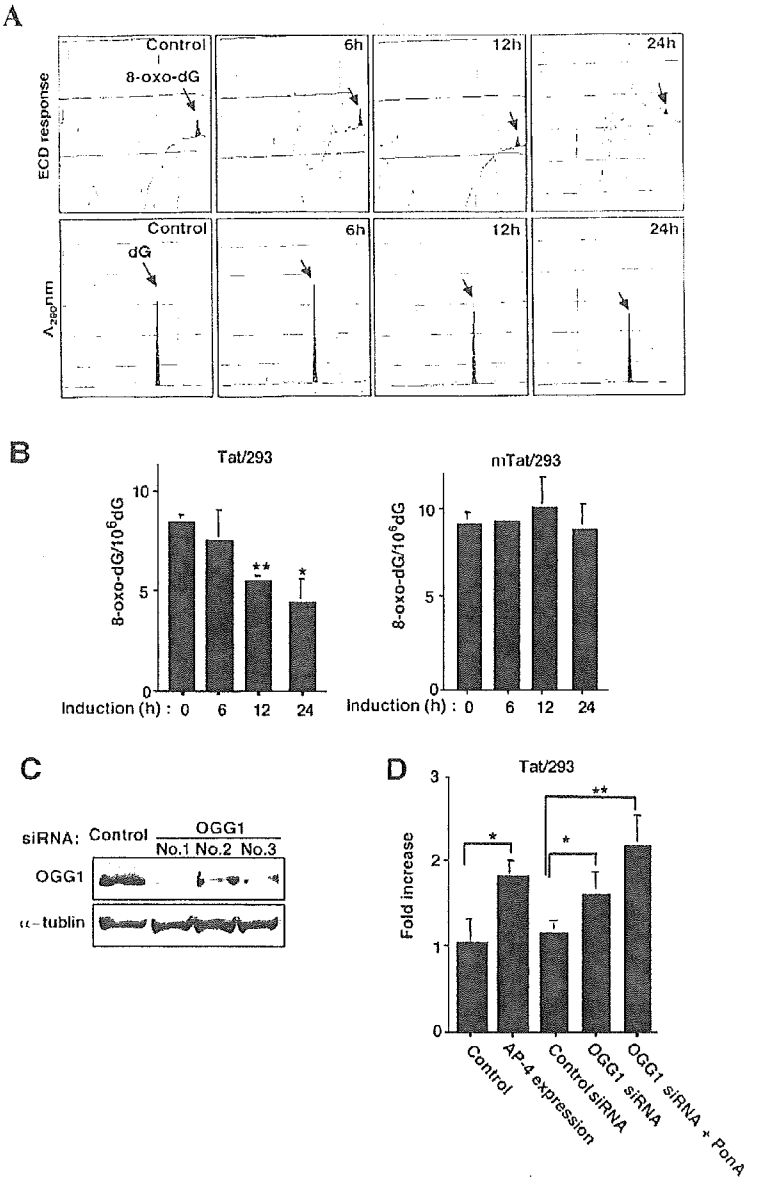

FIG. 7. **Reduction in the levels of 8-oxo-dG by Tat.** *A*, electrochemical chromatographs of 8-oxo-dG. The HPLC patterns were traced using an ECD. The 8-oxo-dG peaks (ECD response; *shaded areas* in the *upper panels*) are indicated by *arrows*. The dG peaks (absorption at 290 nm; *shaded areas* in the *lower panels*) are also indicated. Cells were treated for the indicated periods of time with PonA (10 μM) to express Tat or mTat. Nuclear DNA samples were prepared and measured for 8-oxo-dG levels. DNA was digested to obtain deoxynucleosides and analyzed with an HPLC-ECD system as described under "Experimental Procedures." *B*, levels of 8-oxo-dG in DNA expressing Tat or mTat. The amount of 8-oxo-dG is expressed as the number of 8-oxo-dG residues/10^6 dG residues. The results represent the means ± S.D. from four independent experiments. *, $p < 0.005$; **, $p < 0.001$. *C*, OGG1 knockdown by siRNA. Tat/293 cells were transfected with 100 nM siRNAs directed against various portions of OGG1 (Nos. 1–3) or green fluorescent protein (control) mRNAs. After 72 h of transfection, cells were lysed, and OGG1 protein levels were assessed by Western blotting with anti-OGG1 antibody (*upper panel*). The blot was stripped and reprobed with anti-α-tubulin antibody (*lower panel*). *D*, effects of OGG1 depletion and expression of Tat and AP-4 on the levels of 8-oxo-dG. *First bar*, control Tat/293 cells (no treatment); *second bar*, Tat/293 cells transfected with plasmid expressing AP-4; *third* and *fourth bars*, Tat/293 cells transfected with siRNA against green fluorescent protein (siRNA control) or OGG1 (No. 1), respectively, and incubated for 72 h; *fifth bar*, Tat/293 cells transfected with siRNA against OGG1 (No. 1) for 48 h and treated with PonA to induce Tat expression for an additional 24 h. At 72 h post-transfection, nuclear DNA samples were extracted, and the levels of 8-oxo-dG were measured similarly as described for *A*. The levels of 8-oxo-dG are shown as the -fold increase compared with the level of the no-treatment sample (*first bar*). *, $p < 0.05$; **, $p < 0.01$.

effect of OGG1 mutation on the extent of mutation of viral and cellular genomes during chronic HIV infection, the Tat-mediated induction of OGG1 could be viewed as a regulated "feed-forward" mechanism.

Acknowledgments—We thank Drs. J. P. Radicella and L. Naumovski for providing the plasmid constructs containing various portions of the *OGG1* promoter and 293/LacZ cells, respectively. We also thank A. Victoriano for language revision.

REFERENCES

1. Jones, K. A., and Peterlin, B. M. (1994) *Annu. Rev. Biochem.* **63,** 717–743
2. Berkhout, B., Silverman, R. H., and Jeang, K. T. (1989) *Cell* **59,** 273–282
3. Okamoto, T., and Wong-Staal, F. (1986) *Cell* 29–35
4. Okamoto, H., Sheline, C. T., Corden, J. L., Jones, K. A., and Peterlin, B. M. (1996) *Proc. Natl. Acad. Sci. U. S. A.* **93,** 11575–11579
5. Wei, P., Garber, M. E., Fang, S. M., Fischer, W. H., and Jones, K. A. (1998) *Cell* **92,** 451–462
6. Kanazawa, S., Okamoto, T., and Peterlin, B. M. (2000) *Immunity* **12,** 61–70
7. Mancebo, H. S., Lee, G., Flygare, J., Tomassini, J., Luu, P., Zhu, Y., Peng, J., Blau, C., Hazuda, D., Price, D., and Flores, O. (1997) *Genes Dev.* **11,** 2633–2644
8. Zhu, Y., Pe'ery, T., Peng, J., Ramanathan, Y., Marshall, N., Marshall, T., Amendt, B., Mathews, M. B., and Price, D. H. (1997) *Genes Dev.* **11,** 2622–2632
9. Marzio, G., Tyagi, M., Gutierrez, M. I., and Giacca, M. (1998) *Proc. Natl. Acad. Sci. U. S. A.* **95,** 13519–13524
10. Price, D. H. (2000) *Mol. Cell. Biol.* **20,** 2629–2634
11. Zauli, G., Gibellini, D., Milani, D., Mazzoni, M., Borgatti, P., La Placa, M., and Capitani, S. (1993) *Cancer Res.* **53,** 4481–4485
12. Flores, S. C., Marecki, J. C., Harper, K. P., Bose, S. K., Nelson, S. K., and McCord, J. M. (1993) *Proc. Natl. Acad. Sci. U. S. A.* **90,** 7632–7636
13. Westendorp, M. O., Shatrov, V. A., Schulze-Osthoff, K., Frank, R., Kraft, M., Los, M., Krammer, P. H., Droge, W., and Lehmann, V. (1995) *EMBO J.* **14,** 546–554
14. Conant, K., Garzino-Demo, A., Nath, A., McArthur, J. C., Halliday, W., Power, C., Gallo, R. C., and Major, E. O. (1998) *Proc. Natl. Acad. Sci. U. S. A.* **95,** 3117–3121
15. Izmailova, E., Bertley, F. M., Huang, Q., Makori, N., Miller, C. J., Young, R. A., and Aldovini, A. (2003) *Nat. Med.* **9,** 191–197
16. Choi, J., Liu, R. M., Kundu, R. K., Sangiorgi, F., Wu, W., Maxson, R., and Forman, H. J. (2000) *J. Biol. Chem.* **275,** 3693–3698
17. Kumar, A., Manna, S. K., Dhawan, S., and Aggarwal, B. B. (1998) *J. Immunol.* **161,** 776–781
18. Li, Y., Kappes, J. C., Conway, J. A., Price, R. W., Shaw, G. M., and Hahn, B. H. (1991) *J. Virol.* **65,** 3973–3985
19. Moriyama, E. N., Ina, Y., Ikeo, K., Shimizu, N., and Gojobori, T. (1991) *J. Mol. Evol.* **32,** 360–363
20. Perry, S. T., Flaherty, M. T., Kelley, M. J., Clabough, D. L., Tronick, S. R., Coggins, L., Whetter, L., Lengel, C. R., and Fuller, F. (1992) *J. Virol.* **66,** 4085–4097
21. Vartanian, J. P., Meyerhans, A., Asjo, A., and Wain-Hobson, S. (1991) *J. Virol.* **65,** 1779–1788
22. Harris, R. S., Bishop, K. N., Sheehy, A. M., Craig, H. M., Petersen-Mahrt,

S. K., Watt, I. N., Neuberger, M. S., and Malim, M. H. (2003) *Cell* **113,** 803–809
23. Mangeat, B., Turelli, P., Caron, G., Friedli, M., Perrin, L., and Trono, D. (2003) *Nature* **424,** 99–103
24. Mariani, R., Chen, D., Schrofelbauer, B., Navarro, F., Konig, R., Bollman, B., Munk, C., Nymark-McMahon, H., and Landau, N. R. (2003) *Cell* **114,** 21–31
25. Zhang, H., Yang, B., Pomerantz, R. J., Zhang, C., Arunachalam, S. C., and Gao, L. (2003) *Nature* **424,** 94–98
26. Kasai, H., and Nishimura, S. (1984) *Nucleic Acids Res.* **12,** 2137–2145
27. Kasai, H. (1997) *Mutat. Res.* **387,** 147–163
28. Hatahet, Z., Zhou, M., Reha-Krantz, L. J., Morrical, S. W., and Wallace, S. S. (1998) *Proc. Natl. Acad. Sci. U. S. A.* **95,** 8556–8561
29. Hussain, S. P., and Harris, C. C. (1998) *Cancer Res.* **58,** 4023–4037
30. Boiteux, S., and Radicella, J. P. (2000) *Arch. Biochem. Biophys.* **377,** 1–8
31. Radicella, J. P., Dherin, C., Desmaze, C., Fox, M. S., and Boiteux, S. (1997) *Proc. Natl. Acad. Sci. U. S. A.* **94,** 8010–8015
32. Rosenquist, T. A., Zharkov, D. O., and Grollman, A. P. (1997) *Proc. Natl. Acad. Sci. U. S. A.* **94,** 7429–7434
33. Arai, T., Kelly, V. P., Komoro, K., Minowa, O., Noda, T., and Nishimura, S. (2003) *Cancer Res.* **63,** 4287–4292
34. Minowa, O., Arai, T., Hirano, M., Monden, Y., Nakai, S., Fukuda, M., Itoh, M., Takano, H., Hippou, Y., Aburatani, H., Masumura, K., Nohmi, T., Nishimura, S., and Noda, T. (2000) *Proc. Natl. Acad. Sci. U. S. A.* **97,** 4156–4161
35. Okamoto, H., Cujec, T. P., Okamoto, M., Peterlin, B. M., Baba, M., and Okamoto, T. (2000) *Virology* **272,** 402–408
36. Takada, N., Sanda, T., Okamoto, H., Yang, J. P., Asamitsu, K., Sarol, L., Kimura, G., Uranishi, H., Tetsuka, T., and Okamoto, T. (2002) *J. Virol.* **76,** 8019–8030
37. Dhénaut, A., Boiteux, S., and Radicella, J. P. (2000) *Mutat. Res.* **461,** 109–118
38. Ao, Y., Rohde, L. H., and Naumovski, L. (2001) *Oncogene* **20,** 2720–2725
39. Ando, K., Kanazawa, S., Tetsuka, T., Ohta, S., Jiang, X., Tada, T., Kobayashi, M., Matsui, N., and Okamoto, T. (2003) *Oncogene* **22,** 7796–7803
40. Watanabe, N., Ando, K., Yoshida, S., Inuzuka, S., Kobayashi, M., Matsui, N., and Okamoto, T. (2002) *Biochem. Biophys. Res. Commun.* **294,** 1121–1129
41. Tetsuka, T., Uranishi, H., Imai, H., Ono, T., Sonta, S., Takahashi, N., Asamitsu, K., and Okamoto, T. (2000) *J. Biol. Chem.* **275,** 4383–4390
42. Sarol, L. C., Imai, K., Asamitsu, K., Tetsuka, T., Barzaga, N. G., and Okamoto, T. (2002) *Biochem. Biophys. Res. Commun.* **291,** 890–896
43. Pincus, S. H., Messer, K. G., and Hu, S. H. (1994) *J. Clin. Investig.* **93,** 140–146
44. Tsurudome, Y., Hirano, T., Yamato, H., Tanaka, I., Sagai, M., Hirano, H., Nagata, N., Itoh, H., and Kasai, H. (1999) *Carcinogenesis* **20,** 1573–1576
45. Saez, E., Nelson, M. C., Eshelman, B., Banayo, E., Koder, A., Cho, G. J., and Evans, R. M. (2000) *Proc. Natl. Acad. Sci. U. S. A.* **97,** 14512–14517
46. Buckbinder, L., Velasco-Miguel, S., Chen, Y., Xu, N., Talbott, R., Gelbert, L., Gao, J., Seizinger, B. R., Gutkind, J. S., and Kley, N. (1997) *Proc. Natl. Acad. Sci. U. S. A.* **94,** 7868–7872
47. Kurdistani, S. K., Arizti, P., Reimer, C. L., Sugrue, M. M., Aaronson, S. A., and Lee, S. W. (1998) *Cancer Res.* **58,** 4439–4444
48. Mathupala, S. P., Heese, C., and Pedersen, P. L. (1997) *J. Biol. Chem.* **272,** 22776–22780
49. Li, C. J., Wang, C., Friedman, D. J., and Pardee, A. B. (1995) *Proc. Natl. Acad. Sci. U. S. A.* **92,** 5461–5464
50. Longo, F., Marchetti, M. A., Castagnoli, L., Battaglia, P. A., and Gigliani, F. (1995) *Biochem. Biophys. Res. Commun.* **206,** 326–334
51. Nishioka, K., Ohtsubo, T., Oda, H., Fujiwara, T., Kang, D., Sugimachi, K., and Nakabeppu, Y. (1999) *Mol. Biol. Cell.* **10,** 1637–1652
52. Clark, E., Santiago, F., Deng, L., Chong, S., de La Fuente, C., Wang, L., Fu, P., Stein, D., Denny, T., Lanka, V., Mozafari, F., Okamoto, T., and Kashanchi, F. (2000) *J. Virol.* **74,** 5040–5052
53. Mermod, N., Williams, T. J., and Tjian, R. (1988) *Nature* **332,** 557–561
54. Andriamanalijaona, R., Felisaz, N., Kim, S. J., King-Jones, K., Lehmann, M., Pujol, J. P., and Boumediene, K. (2003) *Arthritis Rheum.* **48,** 1569–1581
55. Cui, Y., Narayanan, C. S., Zhou, J., and Kumar, A. (1998) *Gene (Amst.)* **224,** 97–107
56. Ou, S. H., Garcia-Martinez, L. F., Paulssen, E. J., and Gaynor, R. B. (1994) *J. Virol.* **68,** 7188–7199
57. Staal, F. J., Ela, S. W., Roederer, M., Anderson, M. T., Herzenberg, L. A., and Herzenberg, L. A. (1992) *Lancet* **339,** 909–912
58. Roederer, M., Staal, F. J., Raju, P. A., Ela, S. W., Herzenberg, L. A., and Herzenberg, L. A. (1990) *Proc. Natl. Acad. Sci. U. S. A.* **87,** 4884–4888
59. Kalebic, T., Kinter, A., Poli, G., Anderson, M. E., Meister, A., and Fauci, A. S. (1991) *Proc. Natl. Acad. Sci. U. S. A.* **88,** 986–990

0022-3565/05/3152-624–630$20.00
THE JOURNAL OF PHARMACOLOGY AND EXPERIMENTAL THERAPEUTICS
Copyright © 2005 by The American Society for Pharmacology and Experimental Therapeutics
JPET 315:624–630, 2005

Vol. 315, No. 2
88674/3054193
Printed in U.S.A.

Prevention of the Ultraviolet B-Mediated Skin Photoaging by a Nuclear Factor κB Inhibitor, Parthenolide

Kiyotaka Tanaka, Junichi Hasegawa, Kaori Asamitsu, and Takashi Okamoto

Department of Molecular and Cellular Biology, Nagoya City University Graduate School of Medical Sciences, Nagoya, Japan (K.T., J.H., K.A., T.O.); and Department of Research and Development, Ichimaru Pharcos Co., Ltd., Motosu, Japan (K.T.)

Received April 28, 2005; accepted July 15, 2005

ABSTRACT

The skin photoaging is characterized by keratinocyte hyperproliferation and degradation of collagen fibers, causing skin wrinkling and laxity and melanocyte proliferation that leads to pigmentation. UV is considered to be a major cause of such skin changes. It is well established that nuclear factor κB (NF-κB) is activated upon UV irradiation and induces various genes including interleukin-1 (IL-1), tumor necrosis factor α (TNFα), and matrix metalloprotease-1 (MMP-1). It is also known that basic fibroblast growth factor (bFGF) production is induced by UV and promotes the proliferation of skin keratinocytes and melanocytes. We found that UVB, IL-1, and TNFα induced NF-κB activation and then produced MMP-1 and bFGF in HaCaT keratinocytes and skin fibroblasts. In this experiment, we examined if parthenolide, an NF-κB inhibitor, could block the UVB-mediated skin changes. We found that parthenolide could effectively inhibit the gene expression mediated by NF-κB and the production of bFGF and MMP-1 from cells overexpressing p65, a major subunit of NF-κB. We also found that parthenolide could inhibit the UVB-induced proliferation of keratinocytes and melanocytes in the mouse skin. These findings suggest that NF-κB inhibitors should be useful for the prevention of skin photoaging.

Skin aging is a complex process that involves intrinsic and exogenous causes. Although intrinsic skin aging is associated with other physiological processes and is inevitable, exogenous aging is caused by extrinsic harmful environments and can be prevented. UV is one of the most noxious factors among the harmful environments (Ulrich et al., 2004). UV irradiation induces inflammatory processes in the skin, and the irradiated skin becomes metabolically hyperactive associated with epidermal hyperproliferation and accelerated collagen fiber breakdown. In contrast, physiologically aged skin is usually characterized by a slow decline in many of these processes (Kligman, 1989). The UV-irradiated skin is characterized by fine and coarse wrinkling, roughness, dryness, laxity, and pigmentation (Chung, 2003). Microscopically, these changes can be explained by keratinocyte hyperproliferation and degradation of collagen fibers (Brenneisen et al., 2002), causing skin wrinkling and laxity, and melanocyte proliferation that leads to pigmentation characterized by dysregulation of melanocyte homeostasis and increase in the melanocyte density (Hirobe et al., 2003). The UV-induced production of proinflammatory cytokines, such as interleukin-1 (IL-1) and tumor necrosis factor α (TNFα), has been considered attributable to these changes (Corsini et al., 1997; Yarosh et al., 2000). Similarly, induction of matrix metalloprotease-1 (MMP-1) is responsible for the degradation of collagen fibers (Wlaschek et al., 1994; Barchowsky et al., 2000). In addition, UV irradiation is known to stimulate both keratinocytes and fibroblasts to induce basic fibroblast growth factor (bFGF) that is responsible for the proliferations of melanocytes and keratinocytes.

It is well established that a transcription factor, nuclear factor κB (NF-κB), is activated upon UV irradiation and induces various genes including IL-1 and TNFα, which subsequently stimulate the signal transduction pathway to activate NF-κB, thus conforming a vicious cycle (Okamoto et al., 1997; Saliou et al., 1999). In fact, NF-κB is known to increase MMP-1 in dermis (Bond et al., 1999; Sun et al., 2002; Chung, 2003). It is also reported that UV irradiation induces bFGF production (Sabourin et al., 1993), presumably through NF-κB activation (Wakisaka et al., 2002). Thus, inhibition of the NF-κB activation pathway would block the vicious cycle elicited by UV irradiation and effectively prevent the UVB-mediated cutaneous alterations.

NF-κB is sequestrated in the cytoplasm as an inactive

This work was supported in part by the Ministry of Health, Labor and Welfare (Grant-in-Aid H16-Immunology-001) and by the Ministry of Education, Culture, Sports, Science and Technology of Japan (Grant-in-Aid 16022254).

Article, publication date, and citation information can be found at http://jpet.aspetjournals.org.

doi:10.1124/jpet.105.088674.

ABBREVIATIONS: IL-1, interleukin-1; TNFα, tumor necrosis factor α; MMP-1, matrix metalloprotease-1; bFGF, basic fibroblast growth factor; NF-κB, nuclear factor κB; IκB, inhibitor κB.

complex with a class of inhibitory molecules known as inhibitor κB (IκB). Treatment of cells with a variety of inducers such as IL-1 and TNF-α results in phosphorylation, ubiquitination, and degradation of the IκB proteins (Hayden and Ghosh, 2004). The phosphorylation of IκB is catalyzed by IκB kinase complex. The phosphorylated IκB is subjected to ubiquitination and proteolytic degradation by proteasome. The degradation of IκB exposes the nuclear localization sequence in the remaining NF-κB dimers, followed by the rapid translocation of NF-κB to the nucleus, where it activates the target genes by binding to the DNA regulatory element.

Parthenolide is a sesquiterpene lactone compound and an active substance in medical herb Feverfew (*Tanacetum parthenium*) traditionally used in the treatment of inflammation in Mexico (Heinrich et al., 1998). It was shown that parthenolide blocked the NF-κB activation pathway at multiple levels such as inhibiting IκB kinase activity (Kwok et al., 2001) and DNA binding of NF-κB (Garcia-Pineres et al., 2001). In this study, we examined the effect of parthenolide in blocking the processes of UVB-mediated cutaneous alterations using cultured cell and animal models.

Materials and Methods

Reagents and Plasmids. Parthenolide, recombinant human TNFα, and IL-1 were purchased from Wako Pure Chemicals (Osaka, Japan). Antibodies to bFGF and epidermal growth factor were purchased from R&D Systems (Minneapolis, MN). The reporter plasmid expressing firefly luciferase under the control of NF-κB (pGL3-4κBwt-Luc) was constructed by inserting four tandem copies of the κB sequence (GGGACTTTCC) from HIV-1 enhancer into pGL3-promoter vector (Promega, Madison, WI) as reported previously (Sato et al., 1998; Tetsuka et al., 2000). Construction of the mutant NF-κB reporter plasmid, pGL3-4κBm-luc, containing mutated NF-κB binding sites, was described previously (Tetsuka et al., 2000). Control luciferase reporter plasmids under controls of CRB, pCRE-luc, and AP1, pAP-1-luc, were purchased from Stratagene (La Jolla, CA). The p65-expressing plasmid, pCMV-p65, was described previously (Tetsuka et al., 2000).

Cell Culture. The HaCaT human keratinocyte cell line (Boukamp et al., 1988) was generously provided by N. Fusenig (Deutsches Krebsforschungszentrum, Heidelberg, Germany). HaCaT cells were grown at 37°C in RPMI 1640 medium supplemented with 1% fetal bovine serum, 100 units/ml penicillin, and 100 μg/ml streptomycin. Human normal epidermal melanocytes (Toyobo Engineering, Osaka, Japan) were grown at 37°C in melanocyte basic medium (Toyobo Engineering) supplemented with 1% fetal bovine serum, 100 units/ml penicillin, and 100 μg/ml streptomycin. Human normal fibroblasts (KURABO, Osaka, Japan) were grown at 37°C in Dulbecco's modified Eagle's medium supplemented with 5% fetal bovine serum, 100 units/ml penicillin, and 100 μg/ml streptomycin. Human embryonic kidney 293 cells (Riken, Tsukuba, Japan) were grown at 37°C in Dulbecco's modified Eagle's medium supplemented with 10% fetal bovine serum, 1 mM glutamate, 100 units/ml penicillin, and 100 μg/ml streptomycin. For UVB irradiation, cell culture medium was changed to phosphate-buffered saline and UVB of 280- to 320-nm wavelength was irradiated at a dose of 0.5 mJ/cm^2 using an FL20 S-E sunlamp (Toshiba, Tokyo, Japan). After the UVB irradiation, the fresh medium was supplied for further cultures.

Transfection and Luciferase Assay. Cells were transfected with various plasmids using Fugene-6 transfection reagent (Roche Diagnostics, Basel, Switzerland). Briefly, cells were cultured in 12-well plates, and transfections were performed with 1.5 μl of Fugene-6 transfection reagent/ml culture medium and a total of 0.5 μg of plasmid DNA as previously described (Tetsuka et al., 2000; Uranishi et al., 2001). Control plasmid pUC19 was used to equalize the amount of DNA for each transfection. Fugene-6-DNA complexes were allowed to form for 15 min at room temperature in serum-free medium before being added to the cells. After 24 h of transfection, cells were incubated for additional 24 h and then harvested. The luciferase activity was measured by the luciferase assay system (Promega). The relative light units were determined with a TD-20/20 Luminometer (Promega). Transfection efficiency was monitored by *Renilla* luciferase activity with pRL-TK plasmid containing TK promoter as an internal control. All luciferase activities shown in transient transfection assays were corrected by the internal control activity of *Renilla* luciferase by pRL-TK. The assays were performed in triplicates. The results were presented as the fold increases in luciferase activities (means ± S.D.) relative to the control in three independent transfections.

Melanocyte Growth Assay. To assess the activity promoting the growth of melanocyte in the supernatant of HaCaT cells, pCMV-p65 was transfected into HaCaT cultured in 12-well plates, cultured for 48 h, and the supernatant was obtained. Melanocytes were cultured in 24-well plates, and the supernatant of HaCaT was added to the melanocyte culture at 2:1, continued for an additional 48 h, and the numbers of melanocytes were counted using WST-1 (Roche Diagnostics). To remove bFGF from the HaCaT culture medium, the HaCaT culture supernatant was incubated with the anti-bFGF antibody premixed with 5% Sepharose A beads (Amersham Biosciences AB, Uppsala, Sweden) at 4°C for 4 h.

Quantitative Determination of bFGF and MMP-1. The commercial EIA kits were used to determine the concentrations of bFGF (Cytimmune, College Park, MD) and MMP-1 (Amersham Biosciences AB) according to the suppliers' protocol. All the measurements were performed in triplicates and repeated at least twice.

Mouse Model for the UVB-Irradiated Skin. Twenty male DBA/2 mice 6 weeks of age were subjected to this study. All mice were randomly allocated to the following four groups: UV + parthenolide treatment, UV treatment, parthenolide treatment, and control. For the groups of UV + parthenolide and UV treatments, the heads of mice were locally exposed to UVB of 280 to 320 nm wavelength at a dose of 180 mJ/cm^2 using an FL20 S-E sunlamp every other day for 12 days. For the group of parthenolide treatment, 250 μg/kg parthenolide in saline was injected i.p. every day during the period of UVB irradiation. The same amount of saline was injected to UV treatment and control groups. After 12 days, ears were excised from all subjects. One of the ear specimens of each animal was stored in −80°C for the microscopic observations of melanocytes, and the other ear specimen was paraffin-embedded for the immunohistochemical analysis of MMP-1 and the determination of skin thickness by hematoxylin and eosin staining (H&E staining). The thickness of epidermis was measured using software for image analysis (Win ROOF; Mitani, Fukui, Japan). These animal experiments were performed according to the institutional regulation and were approved by the institutional review board.

Melanocyte Counting. The melanocyte count in skin tissues was determined microscopically according to the method of Hiramoto et al. (2003). The cartilages were manually removed from the excised mouse ear specimen, and the skin tissues were soaked in 2 N NaBr solution at 37°C for 2 h. The epidermal and basal layers were exfoliated from rest of the skin tissue by this procedure, and melanocytes were stained by immersing in 0.1 M phosphate-buffered saline (pH 7.2) containing 0.14% L-DOPA at room temperature for 3 h and counted under a microscope.

Statistical Analyses. The data were collected from at least three independent experiments. Animal experiments were performed with at least five animals per each treatment group. Quantitative data were expressed as the mean ± S.D. Statistical significance was examined by the analysis of variance and the paired Student's *t* test. Differences were considered statistically significant if $p < 0.05$. The levels of statistical significance were indicated as the following: *, $p < 0.05$; **, $p < 0.01$; and n.s., not significant.

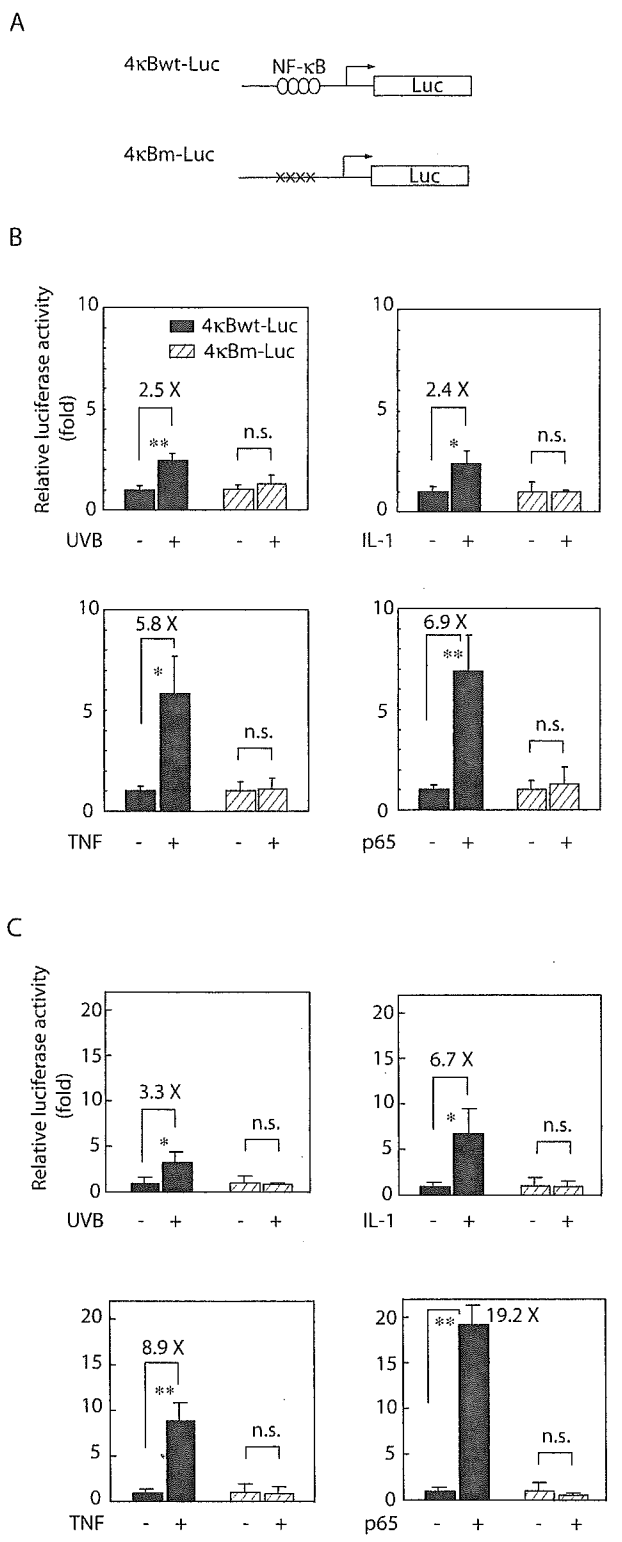

Fig. 1. Induction of the NF-κB-dependent gene expression in cultured human skin cells. A, diagram of reporter gene plasmids. κBwt-luc, luciferase reporter plasmid pGL3 containing four tandem copies of the wild-type NF-κB binding site (GGGACTTTCC); κBm-luc, containing four tandem copies of the mutant NF-κB binding site (CTCACTTTCC). B, NF-κB-dependent gene expression in HaCaT human keratinocyte cell line. C, NF-κB-dependent gene expression in human skin fibroblasts. Experiments were carried out essentially identical to those with HaCaT cells (B). Cells were transfected with κBwt-luc or κBm-luc reporter plasmid, stimulated with UVB (0.5 mJ/cm^2), IL-1 (1.0 ng/ml), or TNFα (1.0 ng/ml). These stimuli were given 24 h after the transfection, and the cell lysates were prepared after additional 24-h incubation for determination of the luciferase activity. As a positive control (denoted as p65), pCMV-p65, expressing the p65 subunit of NF-κB, was cotransfected. As an internal control, pRL-TK, expressing *Renilla* luciferase under the control of TK promoter, was cotransfected. All luciferase activities were corrected by the internal control activity of *Renilla* luciferase. Values (-fold activation) represent the mean ± S.D. of three independent transfections. Similar results were achieved repeatedly. *, $p < 0.05$; **, $p < 0.01$; n.s., not significant.

Results

Induction of NF-κB and the Inhibitory Effects of Parthenolide in Keratinocytes and Fibroblasts. We examined the effects of UVB, IL-1, TNFα, and p65 overexpression on NF-κB dependent gene expression using transient luciferase assay. Since keratinocytes and fibroblasts are major cellular components of the skin, we used human keratinocyte cell line HaCaT as reported previously (Tebbe et al., 2001; Ahn et al., 2003) and primary human fibroblasts. Although UVB cannot penetrate the keratinocyte layer completely, approximately 10% of UVB is known to reach the upper layer of dermis consisting of fibroblasts (Fujisawa et al., 1997). These cells were transfected with luciferase reporter plasmids containing either wild-type κB sites or mutated κB sites, and extents of gene expression were compared in the presence or the absence of these stimuli (Fig. 1).

In HaCaT cells, UVB, IL-1, TNFα, and p65 stimulated gene expression from the reporter plasmid containing NF-κB binding sites by 2.5-, 2.4-, 5.8-, and 6.9-fold, respectively, whereas no significant stimulation was observed when the reporter plasmid containing mutant NF-κB sites was used. Even higher NF-κB-dependent activation was observed in primary fibroblasts. UVB, IL-1, TNFα, and p65 stimulated the luciferase gene expression by 3.3-, 6.7-, 8.9-, and 19.2-fold, respectively. Similar observations were made in 293 cells, a fibroblast cell line derived from human kidney (data not shown). We then examined the effect of parthenolide on the TNFα-mediated NF-κB-dependent gene expression. As shown in Fig. 2, when parthenolide was added to the 293-cell culture, the NF-κB-mediated gene expression was inhibited in a dose-dependent manner for the concentration of parthenolide. In contrast, no such effect of parthenolide was observed on AP-1- or CREB-dependent gene expression. These effects were observed under noncytotoxic concentrations of parthenolide (data not shown).

Induction of bFGF and MMP-1 by NF-κB and the Effects of Parthenolide. The UV-induced cutaneous alterations are known to be mediated by bFGF and MMP-1 (Pittelkow and Shipley, 1989; Chung, 2003). Since it was previously shown that production of bFGF and MMP-1 was induced by UVB (Sabourin et al., 1993; Brenneisen et al., 2002) and that UVB irradiation induced production of IL-1 and TNFα in keratinocytes and fibroblasts (Corsini et al., 1997; Fujisawa et al., 1997), we examined if p65 overexpression, mimicking NF-κB activation, induced production of bFGF and MMP-1. As shown in Fig. 3A, when p65 was overexpressed in keratinocytes and fibroblasts, bFGF production into the culture supernatant was significantly augmented although the transfection efficiency was approximately 3.8 and 9.2% for HaCaT cells and fibroblasts, respectively. Similar effects were observed in the MMP-1 production (Fig. 3B). The amounts of bFGF and MMP-1 production were significantly reduced, almost to the basal level,

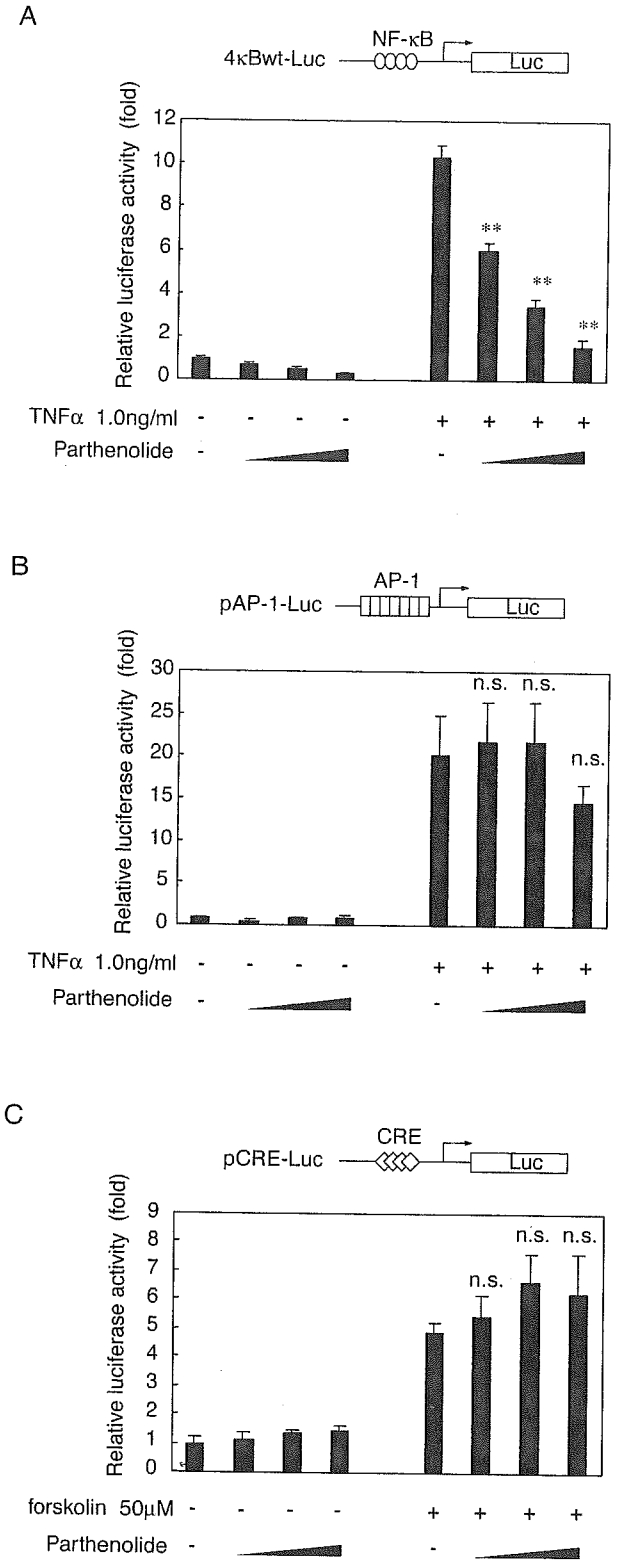

Fig. 2. Inhibition of NF-κB-dependent gene expression by parthenolide. A, effects of parthenolide on NF-κB-dependent gene expression. Experiments were similarly performed as in Fig. 1 except that cells were pretreated with parthenolide at 2.5, 5, or 10 μM of final concentration 2 h prior to the TNFα (1.0 ng/ml) treatment. B and C, effects of parthenolide on gene expression dependent on AP-1 (B) and CREB (C). Parthenolide, at final concentrations of 2.5, 5, or 10 μM, was added 2 h prior to the TNFα or forskolin treatment. Values represent the luciferase activity means ± S.D. of three independent transfections. **, $p < 0.01$; n.s., not significant.

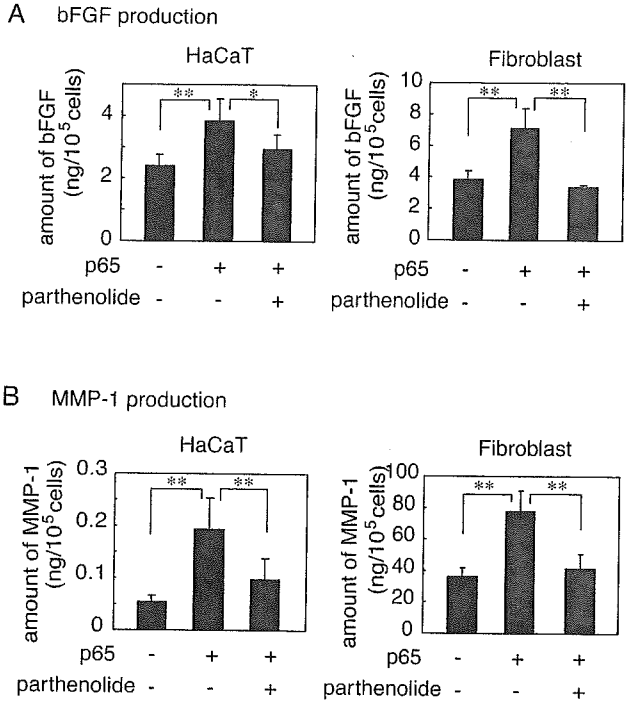

Fig. 3. Effect of NF-κB on production of bFGF and MMP-1 from cultured skin cells and its inhibition by parthenolide. A, effect of NF-κB on production of bFGF. HaCaT or skin fibroblasts were transiently transfected with pCMV-p65, and the culture supernatants were collected after 72 h of transfection for determination of bFGF. Parthenolide (10 μM) was added to each cell culture 24 h after the transfection. The amount of bFGF produced from 10^4 cells was indicated. B, effect of NF-κB on production of MMP-1. HaCaT or skin fibroblasts were transiently transfected with pCMV-p65, incubated for 72 h, and the MMP-1 production in the culture supernatant per 10^4 cells was determined. The inhibitory effect of parthenolide was similarly evaluated. Experiments were performed in triplicate, and the values represent the mean ± S.D. of three independent experiments. Similar results were achieved repeatedly. *, $p < 0.05$; **, $p < 0.01$.

by the treatment with parthenolide. When mice were treated with parthenolide i.p., significant reduction of the MMP production upon UVB irradiation was observed (data not shown), consistent with the results with cultured cells.

Effects of Parthenolide on Epidermal Hyperproliferation and Melanocyte Growth. It is well known that the UV-induced epidermal hyperplasia, consisting of the hyperproliferative keratinocytes and melanocytes (Brenneisen et al., 2002; Chung, 2003; Hirobe et al., 2003) is considered to be due to the action of bFGF induced by UVB (Pittelkow and Shipley, 1989; Bielenberg et al., 1998). In Fig. 4, effects of parthenolide on the UVB-induced epidermal hyperproliferation were shown. UVB (180 mJ/cm^2) was irradiated at the head of mice. Although UVB induced epidermal hyperproliferation by 2.9-fold compared with the control untreated skin, treatment with parthenolide significantly reduced the epidermal hyperproliferation to 1.6-fold.

We then examined the effects of parthenolide on the melanocyte growth (Fig. 5). The epidermal and basal layers were exfoliated from the skin tissue and melanocytes were stained by L-DOPA. As demonstrated in Fig. 5B, although UVB induced melanocyte proliferation by 3.1-fold in the number of melanocytes compared with the control untreated skin, it was significantly reduced by the treatment with parthenolide to 2.1-fold compared with the control.